

FMH606 Master's Thesis 2022
Energy and Environmental Technology

Experimental and computational study of gasification of lignin pellets in a bubbling fluidized bed reactor

Saugata Ghosh

Faculty of Technology, Natural sciences and Maritime Sciences
Campus Porsgrunn

Course: FMH606 Master's Thesis, 2022

Title: Experimental and computational study of gasification of lignin pellets in a bubbling fluidized bed reactor

Number of pages: 55

Keywords: Gasification, Lignin pellets, Biomass, Fluidized Bed, CPFD

Student: Saugata Ghosh

Supervisors: Ramesh Timsina and Britt M. E. Moldestad

External partner: SINTEF Energy

Summary:

Sustainable energy supply and waste management are two of the major challenges of the present time. The proper utilization of the vast resource of renewable biomass is necessary for a sustainable civilization toward the net-zero emission target. To achieve this goal, biomass conversion technologies can contribute with their great potential. Gasification of biomass is such a process that produces product gas that can be utilized for power generation or as a raw material for secondary fuel production. Lignin, an available source of biomass, is the second most prevalent natural polymer. It has the potential to be employed effectively in biofuel production. Experiments on the gasification of lignin in a bubbling fluidized bed reactor were carried out in a pilot-scale reactor at the University of South-Eastern Norway (USN), Porsgrunn. A simulation model based on the Computational Particle Fluid Dynamics (CPFD) method was developed using the commercial software Barracuda VR and the results were compared to the experimental data. The average volume percentage of carbon monoxide, hydrogen, methane and nitrogen were found to be around 15.55%, 13.32%, 4.33% and 51.23% respectively in the experiment for the equivalence ratio (ER) 0.165. The data for the gas compositions were also analyzed at the ER of 0.215 and 0.264. The simulation results agree well with most of the experimental results. The oxygen concentration during the experiment was around 1% which showed some degree of air contamination of the gas samples. Product gas yield (GY), lower heating value (LHV), carbon conversion efficiency (CCE), cold gas efficiency (CGE), and energy rate were calculated to analyze the gasifier performance. Lignin pellets showed acceptable results, with an average carbon conversion of around 38%.

Preface

This thesis report is submitted to the University of South-Eastern Norway (USN) for the fulfillment of the requirements for the course of Master's Thesis (FMH606). This project work has been carried out under the supervision of Doctoral Research Fellow Ramesh Timsina and Professor Britt Margrethe Emilie Moldestad.

The external partner of this project was SINTEF Energy. USN provided the simulation tools for this project: Barracuda VR for the computational fluid dynamics (CFD) simulations. USN gave access to the cold flow models for bubbling fluidized bed (BFB) and a pilot-scale BFB gasification reactor. SINTEF energy was responsible for supplying the Lignin pellets.

I am grateful to my main supervisor Dr Ramesh Timsina and my co-supervisor Professor Britt M. E. Moldestad for their immense guidance, support and motivation throughout the journey. Moreover, I am deeply indebted to their kindness for believing in me consistently. I am also thankful to such great Ph.d research fellows like Rajan Jaiswal and Nastaran Ahmadpour Samani for sharing their knowledge and time and being so supportive.

Porsgrunn, 18.05.2022

Saugata Ghosh

Contents

1	Introduction	9
1.1	Background	10
1.2	Goal and Scope.....	11
1.3	Report Outline	11
2	Literature Study	12
2.1	Lignin Properties	12
2.2	Biomass Gasification	14
3	Theory	17
3.1	Biomass Gasification Process	17
3.1.1	<i>Drying and pyrolysis</i>	18
3.1.2	<i>Oxidation and gasification</i>	18
3.1.3	<i>Char conversion</i>	18
3.2	Bubbling Fluidized Bed (BFB) Gasifier	19
3.3	Modelling of Biomass Gasification	20
3.3.1	<i>CPFD model</i>	21
3.4	Application of Syngas	26
3.4.1	<i>Methanol synthesis</i>	26
3.4.2	<i>Hydrogen production</i>	26
3.4.3	<i>Fischer-Tropsch synthesis</i>	27
3.4.4	<i>Mixed alcohol production</i>	27
4	Materials and Methods	28
4.1	Material selection.....	28
4.2	Cold flow model	30
4.3	Experimental setup of BFB gasifier	31
4.4	Gas sampling	33
4.5	CPFD Simulation Setup.....	34
5	Results and discussion	36
5.1	Experimental results.....	36
5.2	Simulation results.....	40
5.3	Comparative analysis	43
6	Conclusion	46
	References.....	47
	Appendices.....	50
	Appendix A: Calculation of ER for lignin pellets based on air flow rates	50
	Appendix B: Formulation of Lower heating value (LHV), Gas yield (GY), Carbon conversion efficiency (CCE), and Cold gas efficiency (CGE)	51
	Appendix C: Gas chromatograph analysis	52
	Appendix D: Task description	55

List of tables

Table 2-1. Typical values for the composition of straw, softwoods and hardwoods [10]	12
Table 2-2. Product gas composition for beech wood and lignin gasification [23].....	15
Table 3-1. Major reactions during a biomass gasification process [8].....	19
Table 3-2. Pyrolysis gas compositions [34]	24
Table 3-3. Reaction kinetics for air gasification	25
Table 3-4. Reactions for methanol synthesis [19].....	26
Table 3-5. Major reactions for FT synthesis	27
Table 4-1. Biomass Properties for Lignin pellets (standards: Ash-EN 14775, Heating values-EN 14918, Moisture-EN 14774, Ultimate-EN 15408, Volatile-EN 15402).....	29
Table 4-2. Initial and boundary conditions	35
Table 5-1. Gasification performance indicator for lignin pellets	39
Table 5-2. Product gas composition for wood pellets and lignin gasification	45

List of figures

Figure 3-1. Major steps in biomass gasification	17
Figure 3-2. Particle scale mechanism in a BFB gasification reactor	20
Figure 4-1. Lignin pellets.....	28
Figure 4-2. Cold flow model of BFB	30
Figure 4-3. Pilot-scale BFB gasifier with auxiliary connections	31
Figure 4-4. BFB gasification reactor at USN, Porsgrunn	32
Figure 4-5. SRI gas chromatography	33
Figure 4-6. Schematic illustration of the barracuda model, (a) Boundary conditions, (b) Computational grid, (c) Initial particle in the bed.....	34
Figure 5-1. Pressure gradient profile for bed material.	36
Figure 5-2. Sieve analysis process and the particle size profile for the bed material.	37
Figure 5-3. Temperature and pressure inside the reactor	38
Figure 5-4. Product gas composition from experiment.....	39
Figure 5-5. Gas composition along the reactor	40
Figure 5-6. Particle volume fraction at simulation bed hydrodynamics at 50 s.....	41
Figure 5-7. Fluid temperature at simulation bed hydrodynamics at 50 s.....	42
Figure 5-8. Product gas properties with respect to time	43
Figure 5-9. Comparison of average gas species at ER = 0.165	44

Nomenclature

BFB – Bubbling Fluidized Bed

CCE – Carbon Conversion Efficiency

CFD – Computational Fluid Dynamics

CGE – Cold Gas Efficiency

CPFD – Computational Particle Fluid Dynamics

DFB – Dual Fluidized Bed

ER – Equivalence Ratio

GC – Gas Chromatography

GY – Gas Yield

KIT – Karlsruhe Institute of Technology

LHV – Lower Heating Value

LPG – Liquefied Petroleum Gas

MP PIC – Multiphase Particle-In-Cell

PLC – Programmable Logic Controller

TNO – Netherlands Organization for Applied Scientific Research

USN – University of South Eastern Norway

VR – Virtual Reactor

WGS – Water-Gas Shift

1 Introduction

The demand for energy is growing every day and therefore, the necessity for the development of new energy supplies and technologies are increasing. Wood was utilized for heat and power until the discovery of low-cost petroleum and natural gas. However, as petroleum resources are becoming rare and costly, alternative and renewable fuel options are required. Biomass is constantly growing on the planet and will continue to play an important role as a renewable energy source in the future. One of the most investigated fields in the energy sector right now is the development of sustainable heat, power, and transportation fuels from biomass.

The transport sector accounted for nearly one-fourth of worldwide emissions in 2016, among which the road and aviation industries account for 86% [1]. This is because the transportation industry is predominantly powered by fossil fuels. Biomass is a renewable energy source derived from hydrocarbons that has the potential to replace fossil-fuel-based products. It is indicated that biomass has the potential to bridge the gap between today's use of fossil fuels and future electric and battery-powered automobiles [2].

Biomass not only has a wide geographic distribution and sufficient supply, but it also helps to prevent climate change [3]. The energy crisis, along with concerns about rising carbon dioxide levels in the atmosphere, has made biomass a viable "non-greenhouse" energy source. Fossil fuel combustion raises CO₂ levels in the atmosphere, causing climate change. The use of biomass as a source of energy has the potential to reduce CO₂ emissions. Biomass fuels reduces NO_x, SO_x, and heavy metal emissions. Thus, biomass offers a significant potential to meet the world's future energy demands among renewable energy sources.

1.1 Background

Biomass includes more volatile compounds and oxygen than coal. It has a lower carbon content than coal and a higher hydrogen-to-carbon ratio. The three main components of wood-derived biomass are cellulose, hemicellulose, and lignin, as well as modest amounts of extractives.

Lignin is an organic chemical that can be found in a variety of places, including trees and plants. The lignin pellets have a high calorific value and are easy to store. Verdo, a sustainable energy company, discovered a large stock of lignin and wood fiber remnants in Russia a few years ago. After examining the residual product, the company was convinced that the raw material may be a viable alternative biofuel for major energy plants [4].

Gasification is one of the most appealing methods for converting biomass into hydrogen and other products. Biomass gasification is the partial oxidation of biomass into syngas (a mixture of CO and H₂) in the presence of air, oxygen, and/or steam [5]. Biomass such as lignin, wood chips, agricultural waste, and other biomasses can be converted into high-energy product gas through the gasification process. The gasification products can be utilized for power generation in a gas engine, methanol synthesis, or as raw materials for secondary fuels like biodiesel, bio-ethanol, and methanol synthesis [5]. Biofuels can be manufactured and integrated into existing infrastructure [2]. Gasification technology can be integrated to improve the efficiency of existing conventional power plants [6].

Fluidized bed reactors are one of the most used biomass gasification systems. The fluidized bed technology heats the biomass particles at a temperature of 700-1100°C using a bed material such as sand or olivine [7]. Furthermore, the fluidized bed reactor is one of the most appealing technologies for biomass gasification because of its even heat and mass transfer distribution and efficient solid mixing. Various chemical reactions and heat transfer are all the part of the fluidized bed gasification process. Fluidized beds have capacities ranging from 2MW to 100 MW.

For a thorough knowledge of the gasification process, modeling and simulation of such systems are required. The systems that handle fluid flow are modeled using computational fluid dynamics (CFD). The Eulerian approach is used for fluid particles and the Lagrangian

approach is used for solid particles in a modelling called multiphase particle-in-cell (MP PIC). Barracuda VR is a software that uses MP PIC modeling, often known as the Computational Particle Fluid Dynamics (CPFD) method [8].

1.2 Goal and Scope

The main goal of this thesis was to perform gasification of lignin pellets in a bubbling fluidized bed and to develop a CFD model for the same process. The goal can be divided into four primary tasks:

1. Experimental study of the lignin pellets using the gasification reactor located at USN.
2. Analysis of the produced syngas (heating value and carbon conversion) obtained from the experiment.
3. Analysis of gas composition, heating value and carbon conversion and compared with other biomasses.
4. Development of a CPFD model to simulate the same process in Barracuda VR.

1.3 Report Outline

This report contains six chapters. The first chapter includes a brief introduction with the background and objectives of the study. In the second chapter, a literature study is done on lignin properties and biomass gasification. The theory and governing equations are discussed in the third chapter. Methods and materials are presented in detail in the fourth chapter. The fifth chapter discusses the results and comparative study between simulation and experimental data. Finally, the sixth chapter contains the conclusion of this study mentioning some recommendations for further research.

2 Literature Study

This chapter provides an overview of biomass focusing on lignin properties, global production amounts and other possible applications with a literature review of biomass gasification and its application.

2.1 Lignin Properties

Though there is a wide range of sources, the composition of biomass varies significantly. The main components of the biomass are cellulose, hemicelluloses, lignin, starch, and proteins. However, trees, a common example of biomass, consist of cellulose, hemicelluloses, and lignin. Table 2-1, shows typical values of cellulose, hemi-cellulose and lignin for the composition of straw, softwoods and hardwoods [9].

Table 2-1. Typical values for the composition of straw, softwoods and hardwoods [9]

Type	Cellulose (%)	Hemi-cellulose (%)	Lignin (%)
Softwood	45	25	30
Hardwood	42	38	20
Straw stalks	40	45	15

Lignin is the most abundant natural aromatic polymer which is found in most of the terrestrial plants on earth in the range of 15-40% dry weight and provides structural integrity [10]. The phenylpropane units in lignin have characteristic side chains. In solid form, lignin forms an amorphous structure due to some crosslinking [11]. On average, each year, $5-36 \times 10^8$ tons of lignin are produced on Earth [12]. Lignin is manufactured on an industrial scale in factories that produce paper and pulp, as well as in biorefineries. Approximately 50 million tons of lignin are produced annually by the paper and pulping industry alone, but the majority is currently used as a low-cost fuel to balance energy needs [13]. Commercially, only about 1 million tons per year of lignin are used in concrete additives, dyestuff dispersants, binders or

surfactants for animal feed, dust control, and pesticides [14]. Nevertheless, the market demand for all these non-fuel lignin uses represents a negligible proportion of current lignin production. The major challenge for the commercialization of high-performance lignin products is that lignin has heterogeneous properties, such as molecular weight, functionality, and thermal properties, which may result from different sources and processing methods [15]. Therefore, the development of high-performance lignin-derived materials should be pursued for the development of new applications for lignin.

According to Sannigrahi et al. [16], biofuels made from cellulosic materials have renewed the focus on lignin chemistry. A lignin-rich solid residue is produced in all bioconversion platforms for ethanol production from lignocellulosic biomass. This solid stream is primarily composed of lignin but may contain other elements that require purification before being converted into lignin based materials. There are currently several pathways available for converting this lignin-rich solid residue into liquid fuels which include fragmentation, hydro-processing and thermal depolymerization. Lignin research is sure to gain prominence in the second millennium as the cellulosic biofuels research was dominated in the first decade of the new millennium [16].

The research and development activities aimed at commercializing cellulosic ethanol, have opened up opportunities for increasing the value of lignin [10]. In this study, the recent advances in the lignin valorization effort are highlighted. In recent years, genetic variations discovered in native populations of bioenergy crops, and direct manipulations of biosynthesis pathways have produced lignin feedstocks with favorable properties for recovery and downstream conversion. Analysis of the structure and computational modeling of modified lignin enables direct bioengineering strategies to optimize future properties. In addition to the refinement of biomass pretreatment technologies, genetic engineering will enable new uses for this biopolymer, such as low-cost carbon fibers, engineered plastics and thermoplastic elastomers, polymeric foams, fungible fuels, and commodity chemicals [10].

The aromatic structure of lignin makes it a promising platform or precursor for obtaining value-added compounds [17]. However, for the pulping industry, lignin is generally considered to be a low-value byproduct or fuel. This literature review showed that lignin can be used as a byproduct to get value-added chemicals. New technologies are being developed

to produce carbon and polymer materials from lignin. Furthermore, the technical, economic, and environmental aspects of lignin processing at different stages of biorefinery were described well. Therefore, This study discusses lignin valorization processes in the light of current studies. For a better understanding of the importance of lignin as a platform product in biorefineries, a preliminary techno-economic and environmental assessment of a wood-based biorefinery were conducted here. The review demonstrated that lignin valorization can increase biorefineries' efficiency and sustainability [17].

2.2 Biomass Gasification

The process of biomass gasification involves partial oxidation of biomass to produce syngas (a mixture of CO and H₂), in a limited supply of air, oxygen, and/or steam [18]. CO₂ and CH₄ are byproducts of the biomass gasification process [7].

A literature study shows that several experiments have been done on biomass gasification. Campoy et al. [19] investigated the biomass gasification behavior in a bubbling fluidized bed (BFB) using wood pellets with air and air/steam as a gasifying agent. Experiments were carried out with various biomass and steam flow rates at constant air flow rates. To maintain an appropriate temperature level in the reactor, biomass throughput was reduced as steam addition increased. When the equivalence ration (ER) was altered from 0.19 to 0.35 in pure air gasification, the gas composition and yield varied between 18.2-15.8% CO, 13.2-8.7% H₂, 6-4.6% CH₄, and 0.6-1.2 Nm³/kg of biomass, respectively. The addition of steam resulted in more H₂ in the product gas, but the plant efficiency improved linearly as ER increased. Later, the pilot plant was modified by adding an auxiliary electrical heating system [20], and O₂ enhanced air-steam mixes were tested. With a maximum lower heating value (LHV) of 8 MJ/Nm³, the CO and H₂ levels climbed to 25% and 27%, respectively.

Liakakou et al. [21] described the use of lignin-rich wastes from second-generation bioethanol production to produce syngas that can be used in the gas fermentation process. The authors performed three different gasification studies at different scales. Fixed bed updraft gasification with a solid feed rate of about 30 kg/h, bubbling fluidized bed gasification with a solid feed rate of about 0.3 kg/h, and indirect gasification with a solid feed rate of about 3 kg/h. The results were examined in terms of feedstock pretreatment (grinding, drying, and

pelleting) and syngas quality. It showed that low H₂ to CO ratios are preferable for syngas fermentation because most organisms grow better on CO than H₂ [21].

Liakakou et al. [22] have performed another experiment in an indirect gasifier at TNO (Netherlands Organization for Applied Scientific Research), where a lignin-rich feedstock was gasified using steam. The gas contained CO, H₂, CO₂, CH₄, N₂, C₂H₆, and traces of some other hydrocarbons. The effect of the resulting syngas quality and composition on the fermentation process was investigated at KIT (Karlsruhe Institute of Technology). In the fermentation process, product gas from beech wood gasification was also examined under the same conditions and then compared with the performance of lignin [22]. Table 2-2 gives the overview of the product gases from beech wood and lignin.

Table 2-2. Product gas composition for beech wood and lignin gasification [22]

Gas component	Beech wood (%)	Lignin (%)
CO	31.2	20
H ₂	31.8	35.8
CO ₂	22.4	24.2
CH ₄	9.2	11.4
N ₂	1.3	1.4

In order to acquire a better understanding of the fluid dynamics in a bubbling fluidized bed gasifier, Furuvik et al. [23] combined experimental and computational research. The goal was to create a Computational Particle Fluid Dynamic (CPFD) model that might be used in future studies of the relationship between flow behavior and bed agglomeration in fluidized beds during biomass gasification. The pilot-scale gasifier is located at the University of South-Eastern Norway (USN) and has a capacity of 20 kW. The computational analysis was conducted using the commercial CPFD program Barracuda Virtual Reactor (VR). The CPFD model was validated by comparing simulation results to experimental data. The simulations

predicted pressure drops that were very close to the experimental results, indicating that the model is capable of analyzing fluid dynamics in a fluidized bed system [23].

In 2021, Timsina et al. [24] performed experiments on the gasification of wood pellets and grass pellets in the BFB gasification reactor. The experiment was carried out in the same laboratory-scale bubbling fluidized bed system at USN. Wood and grass pellets were gasified at temperatures ranging from 750 to 900°C at atmospheric circumstances. The product gas compositions and gasifier performance were measured and studied at various equivalence ratios. Product gas yield, LHV, carbon conversion efficiency (CCE), cold gas efficiency (CGE), and energy rate were used to calculate gasifier performance. Wood pellets showed acceptable results, with a carbon conversion of around 60% at a temperature of roughly 850°C [24].

3 Theory

3.1 Biomass Gasification Process

Gasification is one of the efficient methods for producing hydrogen from biomass. Biomass gasification is the process of converting biomass into a gaseous product that primarily contains hydrogen (H_2) and carbon monoxide (CO), with carbon dioxide (CO_2), oxygen (O_2), methane (CH_4) and nitrogen (N_2). The mixture of CO and H_2 is called synthesis gas. The gasification process is carried out in the presence of a gasifying agent like air, oxygen, or steam.

Depending on the fuel type, gasifier type, and operating conditions, multiple physical, chemical, and thermal processes may occur simultaneously or sequentially as the biomass enters the reactor. Figure 3-1 [18] illustrates the essential processes in the biomass gasification process and the steps are described below.

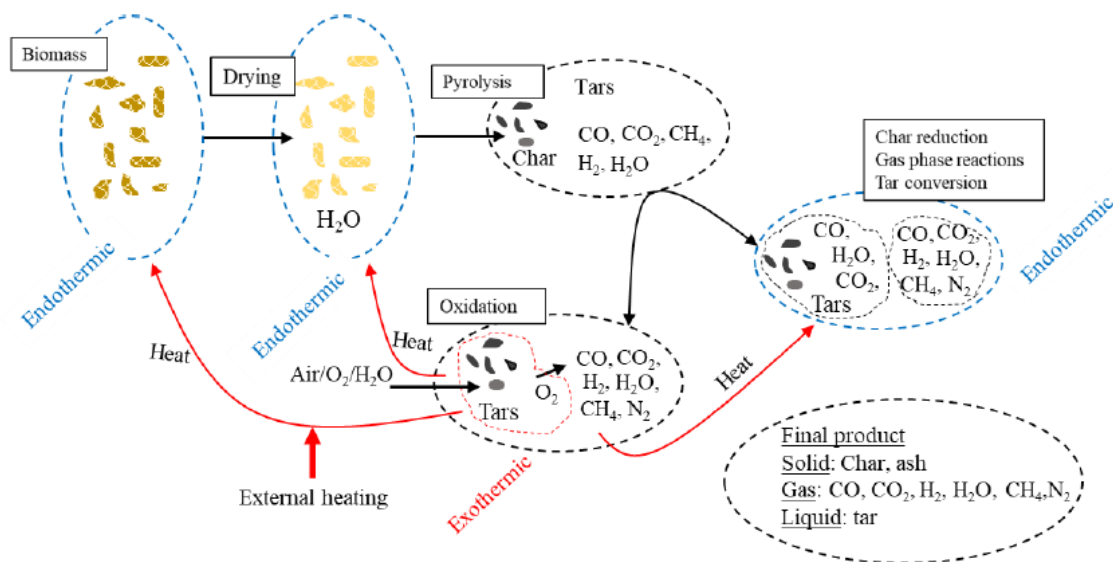
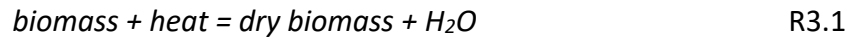


Figure 3-1. Major steps in biomass gasification

3.1.1 Drying and pyrolysis

Moisture is the first component to vaporize when biomass enters operating gasifiers.



Pyrolysis or devolatilization occurs when the temperature of the dry biomass rises to roughly 300-400°C, converting the dry biomass to char, tar, and volatiles [25]. The volatiles goes through a sequence of homogenous reactions both within the bed and in the freeboard zone.



3.1.2 Oxidation and gasification

As an oxidizing agent, a limited amount of oxygen is supplied into the gasifier. To provide the thermal energy required for the gasification reactions, a certain proportion of the product generated (char) during the devolatilization process is oxidized. Char can be gasified by H₂O and CO₂ at temperatures above 700°C. At high pressure, H₂ can be used to gasify char. Heterogeneous gasification reactions are much slower than devolatilization and oxidation reactions, allowing for better control of product generation [25]. Simultaneously, a homogenous reaction takes place between the various gases present inside the reactor. The water gas shift (WGS) reaction is one of the most essential reactions in the gasification process. The WGS reaction can be utilized to adjust the ratio of H₂ and CO in the product gas.

3.1.3 Char conversion

In comparison to the devolatilization step, char conversion or char reactivity is a slow process that is often addressed as a rate-limiting step in a gasification process. The rate of reaction is determined by the type of carbonaceous material being reacted, its surface area, and the activation energy associated with it. The reactivity of char [26] can be expressed as :

$$r_m = -\frac{1}{m_c} \frac{dm_c}{dt} = \frac{1}{(1-x_c)} \frac{dx_c}{dt} \quad 3.1$$

Where, m_c is the mass of carbon contained in the sample and x_c is its conversion rate at time t .

Table 3-1 depicts the primary reactions that occur throughout the biomass gasification process [7].

Table 3-1. Major reactions during a biomass gasification process [7]

Reaction	Name	Enthalpy (KJ/mol)
<i>Heterogeneous reactions</i>		
$C(s) + 0.5O_2 \rightarrow CO$	Char partial oxidation	-111
$C(s) + H_2O \leftrightarrow CO + H_2$	Steam gasification	+131
$C(s) + CO_2 \leftrightarrow 2CO$	Boudouard reaction	+172
$C(s) + 2H_2 \leftrightarrow CH_4$	Methanation	-75
$C(s) + O_2 \rightarrow CO$	Char combustion	-394
<i>Homogeneous reactions</i>		
$H_2 + 0.5O_2 \rightarrow H_2O$	H ₂ oxidation	-242
$C(s) + 0.5O_2 \rightarrow CO_2$	CO oxidation	-283
$CH_4 + 1.5O_2 \rightarrow CO + 2H_2O$	CH ₄ oxidation	
$CO + H_2O \leftrightarrow CO_2 + H_2$	Water-gas shift	-41
$CH_4 + H_2O \leftrightarrow CO + 3H_2$	Methane reforming	+206

3.2 Bubbling Fluidized Bed (BFB) Gasifier

Bubbling fluidized consists of a cylindrical reactor filled with solid bed material for uniform mixing and heat transfer into the biomass particles. A fluidizing agent is introduced from the bottom of the bed to keep the bed in the bubbling fluidization regime. The fluidizing agent contains a limited amount of oxygen (air, steam or pure oxygen) to gasify the biomass particles in the reactor.

The bubbling fluidized bed operates in the temperature range of 700-1100°C [27]. To reduce particle elutriation, the superficial velocity is normally kept at approximately double the minimum fluidization velocity.

The particle scale mechanism in a BFB gasification reactor is illustrated in Figure 3-2 [18].

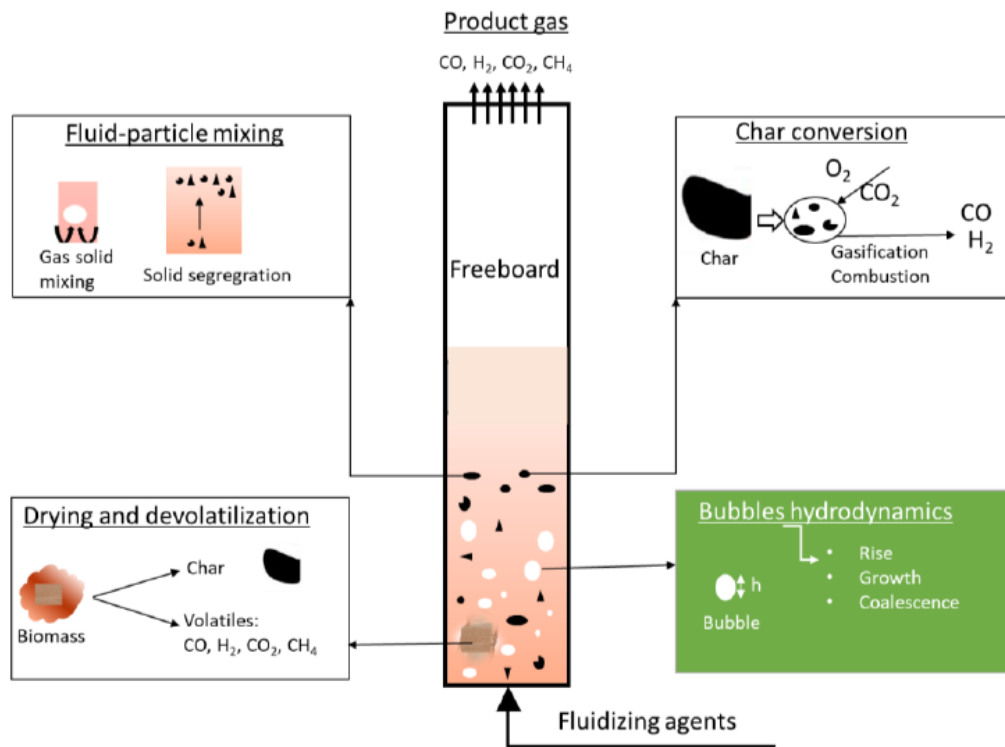


Figure 3-2. Particle scale mechanism in a BFB gasification reactor

In a BFB gasifier, biomass is fed from the top or side of the bed and several complex physical and chemical reactions occur over time and space. The hydrodynamics of the solid bed is influenced by bubbles rising through the solid bed and circulating solids. In a BFB, the random mixing and high heat capacity of the bed material result in a greater rate of heat transfer to the biomass particles under optimal conditions. The gasification behavior of the BFB gasification reactor is heavily influenced by bubble hydrodynamics, particle-particle, and fluid-particle mixing [18].

3.3 Modelling of Biomass Gasification

Modelling the biomass gasification process is difficult due to the combination of turbulent gas flow and particle movements with inter-particle collisions. The basic modelling approaches

are: (i) thermodynamic equilibrium models, (ii) kinetic rate models and (iii) Artificial Neural Network (ANN) models [28].

Computational fluid dynamics (CFD) simulation of biomass gasification incorporates kinetic model theory as well as reactor hydrodynamics. The most frequent methodologies to model the gasification systems are the Eulerian-Eulerian (EE) and Eulerian-Lagrangian (EL) techniques [18].

In the EE technique, both the solid and gas phases are regarded as continuous phases and solved using the Navier-Stokes' equation. This method is also referred to as a two-fluid model, because each phase is distinguished by its volume percent. The approach is extensively used for modeling gas-solid systems because it requires less computer resources. The discrete nature of solid particles and precise transient information about two-phase interactions are missing from the EE technique [29].

The discrete nature of particles is preserved in the EL technique, which models each solid particle using Newton's law of motion in Lagrangian coordinates. The Navier-Stokes' equations are used to simulate the gas phase, which is treated as a continuous phase. This method assumes that the solid phase may interchange mass, momentum, and energy with the fluid phase, implying that the two phases are strongly coupled. Every particle's route is calculated at a predetermined period. Because of the large number of particles in the system and the need for small-time steps to solve particle collisions, the EL approach possesses a heavy load on a computer's central processing unit [30].

3.3.1 CPFD model

A numerical approach for describing particle-fluid and particle-particle interactions in a CFD simulation is the multiphase particle-in-cell method (MP-PIC). The commercial program Barracuda virtual reactor is based on MP-PIC modeling. This modeling is based on the EL method, which decreases the computational costs associated with discrete solid particle modeling [18]. Computational particle fluid dynamics (CPFD) modeling is another name for MP-PIC modeling. Barracuda VR has a high level of accuracy and a short calculation time because of the close interaction between the fluid and particle phases. Because of the rapid advancement of the visual process unit in computers, the CPFD simulation can now simulate

the genuine process in a short amount of time. The main benefit of CPFD is that it can reduce a large commercial plant's billions of particles to millions of computational particles [31]. For solving dense phased gas-solid flow, the CPFD technique is very recent and well appreciated. In three-dimensional Cartesian coordinates, CPFD modeling solves the solid and fluid conservation equations.

3.3.1.1 Governing Equations

The continuity and Navier-Stokes equations represent the mass and momentum conservation equations in the gas phase. Those can be expressed by the following equations:

$$\frac{\partial(\alpha_g \rho_g)}{\partial t} + \nabla \cdot (\alpha_g \rho_g \vec{u}_g) = \delta \dot{m}_p \quad 3.2$$

$$\frac{\partial}{\partial t} (\alpha_g \rho_g \vec{u}_g) + \nabla \cdot (\alpha_g \rho_g \vec{u}_g \vec{u}_g) = -\nabla p + F + \alpha_g \rho_g g + \nabla \cdot (\alpha_g \tau_g) \quad 3.3$$

Where the volume fraction, density, and velocity vector for the gas phase are represented by α_g , ρ_g and \vec{u}_g , respectively. The gas mass production rate per volume generated by the particle-gas chemical reaction is denoted by $\delta \dot{m}_p$. The gravitational acceleration is g , τ_g is the fluid phase stress tensor, F is the inter-phase momentum transfer rate per unit volume (particle to fluid phase) and p is the mean flow gas pressure.

For each gas species, a fluid-phase transport equation is solved. The mass fraction $Y_{g,i}$ of the gas species is used to calculate the fluid phase characteristics. $\delta \dot{m}_{i,c}$ is a chemical source term that refers to the mass transferred between gas species as a result of the dissociation and association of chemical bond. D_t is the turbulent mass diffusivity and can be calculated by Schmidt number's (Sc) correlation. The standard value of Sc is 0.9 [32].

$$\frac{\partial}{\partial t} (\alpha_g \rho_g Y_{g,i}) + \nabla \cdot (\alpha_g \rho_g Y_{g,i} \vec{u}_g) = \nabla \cdot (\alpha_g \rho_g D_t \nabla Y_{g,i}) + \delta \dot{m}_{i,c} \quad 3.4$$

$$\frac{\mu}{\rho_g D} = Sc \quad 3.5$$

The energy conversion of the gas phase can be represented as

$$\begin{aligned} & \frac{\partial}{\partial t} (\alpha_g \rho_g h_g) + \nabla \cdot (\alpha_g \rho_g h_g \vec{u}_g) \\ & = \alpha_g \left(\frac{\partial P}{\partial t} + \vec{u}_g \cdot \nabla P \right) + \varphi - \nabla \cdot (\alpha_g \vec{q}) + \dot{Q} + S_h + \dot{q}_D + q_{wp} \end{aligned} \quad 3.6$$

where h_g is the enthalpy, φ is the viscous dissipation, \dot{Q} is energy source per unit volume, S_h is the conservative energy exchange from the particle to gas phase, \dot{q}_D is the enthalpy diffusion term, \vec{q} is the gas heat flux and q_{wp} is the radiative heat transfer between the thermal wall and the particle phase.

Drag models are critical in multiphase simulations for forecasting hydrodynamics. The model determines the force acting on a particle as a function of particle, fluid, and flow variables. The drag force for a system based on a single particle can be expressed by

$$F_p = m_p D(\vec{u}_g - \vec{u}_p) \quad 3.7$$

Here, D is the drag function which depends on the Reynolds number (Re) and \vec{u}_p is the particle velocity. Also, drag coefficient (C_d) can be defined as the function of Reynolds number [33]. The expressions for the drag function and the Reynolds number can be expressed as

$$D = \frac{3 C_d \rho_g |\vec{u}_g - \vec{u}_p|}{8 \rho_p r_p} \quad 3.8$$

$$Re = \frac{2 \rho_g r_p |\vec{u}_g - \vec{u}_p|}{\mu_g} \quad 3.9$$

where, ρ_p is the particle density, r_p is the particle radius and μ_g is the viscosity of gas phase.

3.3.1.2 Reaction Chemistry

In industrial processes, chemical reactions are very important, and they are directly linked to fluid-particle dynamics. A heterogeneous reaction, for example, produces or consumes gases from solids and changes the overall gas volume and hydrodynamics of the reactor in the end. The reaction rates are also affected by the reactor temperature, which influences the heat and mass transfer as well as the reactor hydrodynamics [32].

Table 3-2 [34] shows the volatile composition based on the pyrolysis gas composition. Fixed carbon, volatile matter, and ash were used to model biomass as virtual elements.

Table 3-2. Pyrolysis gas compositions [34]

Components	Molar fraction (dry basis)
Methane (CH ₄)	0.1213
Carbon monoxide (CO)	0.6856
Carbon-dioxide (CO ₂)	0.1764
Hydrogen (H ₂)	0.0167

Kinetic equations for both heterogeneous and homogeneous reactions were defined using mass action kinetics. During the modeling phase, five significant global homogeneous and heterogeneous reactions were investigated, as shown in Table 3.1. Rate coefficient can be defined as

$$k = Am_s e^{\frac{-E_a}{RT}} \quad 3.10$$

Here, A is Arrhenius constant, E_a is the activation energy, R is the universal gas constant, T is the absolute gas temperature for homogeneous reactions and solid-gas film temperature for heterogeneous reactions and $m_s = \alpha_p \rho_p$ is the solid mass of free carbon per unit cell volume [32].

The reaction kinetics are obtained from several sources in the literature. Table 3-3 provides the reaction kinetics that were used in this study.

Table 3-3. Reaction kinetics for air gasification

Name	Reactions	Reaction rate (mol. m ⁻³ . s ⁻¹)
Char partial oxidation [35]	$C(s) + 0.5O_2 \rightarrow CO$	$2.51 \times 10^{-3} m_s T \exp\left(\frac{-8996}{T}\right) [O_2]$
Steam gasification [32]	$C(s) + H_2O \rightarrow CO + H_2$	$1.272 m_s T \exp\left(\frac{-22645}{T}\right) [H_2O]$
	$C(s) + H_2O \leftarrow CO + H_2$	$1.044 \times 10^{-4} m_s T^2 \exp\left(\frac{-6319}{T} - 17.29\right) [H_2][CO]$
Boudouard reaction [32]	$C(s) + CO_2 \rightarrow 2CO$	$1.272 m_s T \exp\left(\frac{-22645}{T}\right) [CO_2]$
	$C(s) + CO_2 \leftarrow 2CO$	$1.044 \times 10^{-4} m_s T^2 \exp\left(\frac{-2363}{T} - 20.92\right) [CO]^2$
Methanation [32]	$C(s) + 2H_2 \rightarrow CH_4$	$1.368 \times 10^{-3} m_s T \exp\left(\frac{-8078}{T} - 7.087\right) [H_2]$
	$C(s) + 2H_2 \leftarrow CH_4$	$0.151 m_s T^{0.5} \exp\left(\frac{-13578}{T} - 0.372\right) [CH_4]^{0.5}$
H ₂ oxidation [36]	$H_2 + 0.5O_2 \rightarrow H_2O$	$5.69 \times 10^{14} \exp\left(\frac{-17610}{T}\right) [H_2][O_2]^{0.5}$
CO oxidation [37]	$CO + 0.5O_2 \rightarrow CO_2$	$5.62 \times 10^{12} \exp\left(\frac{-16000}{T}\right) [CO][O_2]^{0.5}$
CH ₄ oxidation [36]	$CH_4 + 1.5O_2 \rightarrow CO + 2H_2O$	$5.0118 \times 10^{14} \exp\left(\frac{-24357}{T}\right) [CH_4]^{0.7} [O_2]^{0.8}$
Water-gas shift [32]	$CO + H_2O \rightarrow CO_2 + H_2$	$7.68 \times 10^{10} \exp\left(\frac{-36640}{T}\right) [CO]^{0.5} [H_2O]$
	$CO + H_2O \leftarrow CO_2 + H_2$	$6.4 \times 10^9 \exp\left(\frac{-39260}{T}\right) [H_2]^{0.5} [CO_2]$
Methane reforming [38]	$CH_4 + H_2O \rightarrow CO + 3H_2$	$3 \times 10^5 T \exp\left(\frac{-15042}{T}\right) [CH_4][H_2O]$
	$CH_4 + H_2O \leftarrow CO + 3H_2$	$0.0265 T \exp\left(\frac{-32900}{T}\right) [CO][H_2]^2$

3.4 Application of Syngas

One of the most important features of the biomass gasification process is the potential application of the produced syngas. Methanol synthesis, Hydrogen production, Fischer-Tropsch synthesis, and mixed alcohol production are among the important applications in the field of biofuels.

3.4.1 Methanol synthesis

Methanol, commonly known as methyl alcohol or wood spirits, is a common industrial chemical that can be used as a transportation fuel, blended into other fuels, or processed into other hydrocarbons [39]. Methanol is also used to make formaldehyde, acetic acid, methyl tertiary butyl ether, and gasoline. Methanol is made by hydrogenating carbon oxides in the presence of a suitable catalyst, such as copper oxide, chromium oxide, or zinc oxide. Methanol synthesis reactors need a certain CO/CO₂:H₂ ratio. Obtaining the appropriate ratio from a gasifier is not easy [39]. The ratio must be adjusted to a larger hydrogen content, which is often accomplished through a water gas shift reaction. The stoichiometric reaction is given below in Table 3-4 [18].

Table 3-4. Reactions for methanol synthesis [18]

Reaction	Enthalpy (KJ/mol)
$\text{CO} + 2\text{H}_2 \rightleftharpoons \text{CH}_3\text{OH}$	-90.64
$\text{CO}_2 + 3\text{H}_2 \rightleftharpoons \text{CH}_3\text{OH} + \text{H}_2\text{O}$	-49.67
$\text{CO}_2 + \text{H}_2 \rightleftharpoons \text{CO} + \text{H}_2\text{O}$	+41

3.4.2 Hydrogen production

One of the most promising future energy sources is hydrogen fuel. Biomass gasification produces hydrogen at a lower cost than steam reforming of natural gas [40]. On a volume basis, H₂ production from a dual fluidized bed steam gasification with CO₂ adsorption and proper catalysts can reach up to 70% [41].

3.4.3 Fischer-Tropsch synthesis

The catalytic conversion of syngas into a wide spectrum of hydrocarbon compounds is the basis of Fischer-Tropsch (FT) synthesis. The major products of the FT synthesis are N-paraffins and 1-olefins. The following Table 3-5 can be used to depict the major reactions that occur throughout an FT synthesis. Because of their low aromaticity and lack of Sulphur, the fuels produced by FT synthesis are of high quality. Through FT synthesis, products like LPG, gasoline, jet fuel, and diesel fuels can be obtained [42].

Table 3-5. Major reactions for FT synthesis

Reaction	Name
$(2n + 1)H_2 + nCO \rightarrow C_nH_{(2n+2)} + nH_2O$	Paraffins
$2nH_2 + nCO \rightarrow C_nH_{2n} + nH_2O$	Olefins
$CO + H_2O \rightleftharpoons CO_2 + H_2$	Water-gas shift reaction

3.4.4 Mixed alcohol production

Mixed alcohols are key additives to gasoline that raise the octane number and hence lower vehicle emissions. Mixed alcohol improves the catalyst's resistance to Sulphur poisoning, resulting in simpler gas cleaning facilities. Mixed alcohols and methanol are created jointly, depending on the process parameters and catalysts. Dehydration and oligomerization can also be used to transform mixed alcohols into higher-quality fuels [39].

4 Materials and Methods

Experiments were carried out in a pilot-scale BFB gasification reactor at USN Porsgrunn. This chapter gives an overview of the material selection, the cold flow model for a bubbling fluidized bed, the pilot-scale BFB gasifier and a gas sampling chromatograph.

4.1 Material selection

Lignin pellets supplied by the SINTEF Energy were used as feedstocks for the experiments. The pellets had an average diameter of roughly 6 mm and the length were not uniform. The pellets were analyzed in the Eurofins testing facility. Table 4-1 shows the proximate analysis, ultimate analysis and LHV for the lignin pellets. Figure 4-1 shows the lignin pellets used for this experiment.



Figure 4-1. Lignin pellets

Table 4-1. Biomass Properties for **Lignin** pellets (standards: Ash-EN 14775, Heating values-EN 14918, Moisture-EN 14774, Ultimate-EN 15408, Volatile-EN 15402)

Proximate analysis (wt.%, wet basis)	
Fixed carbon	25.68
Volatiles	65.8
Moistures	8.2
Ash	0.32
Ultimate analysis (wt.%, dry basis)	
Ash	0.32
C	54.8
H	6.3
N	0.78
S	0.11
Cl	0.01
O (by difference)	37.68
LHV (MJ/kg, dry)	23.512

4.2 Cold flow model

The laboratory scale cold flow model of the BFB reactor is shown in Figure 4-2. The cold flow model consists of a cylindrical reactor, airflow supply, and pressure measurement sensors. The air flow meter and the pressure sensor are connected to a computer program available in the setup.

For various airflow rates, the pressure sensors measure the pressure within the bed. The data collected by the pressure sensors on the column's wall is monitored via a LabVIEW program. Compressed air is supplied from the bottom of the bed at room temperature. The supplied air passes through a porous plate for uniform distribution of airflow inside the bed. A digital air flow meter attached to the facility's computer controls the airflow rate. A transparent plastic cylinder with a height of 1.5 m and a diameter of 0.084 m serves as the reactor. The second pressure sensor is located 0.035 m above the air distributor and the corresponding pressure measurements sensors are located at 0.1 m distance apart. USN gave access to this cold flow model for BFB where the minimum fluidization velocity of bed material was investigated.

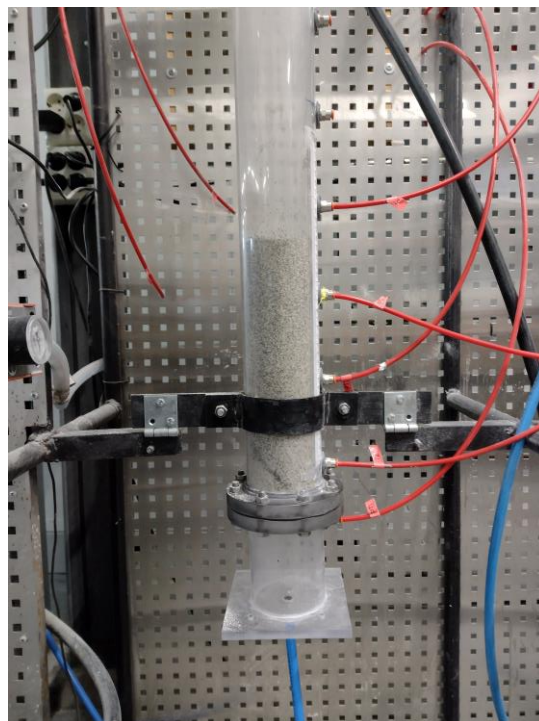


Figure 4-2. Cold flow model of BFB

4.3 Experimental setup of BFB gasifier

Experiments were carried out at the University of South-Eastern Norway, Porsgrunn, in a pilot-scale fluidized bed gasification reactor. The isometric view of the BFB gasifier with auxiliary connections is shown in Figure 4-3. The gasification reactor is depicted in Figure 4-4.

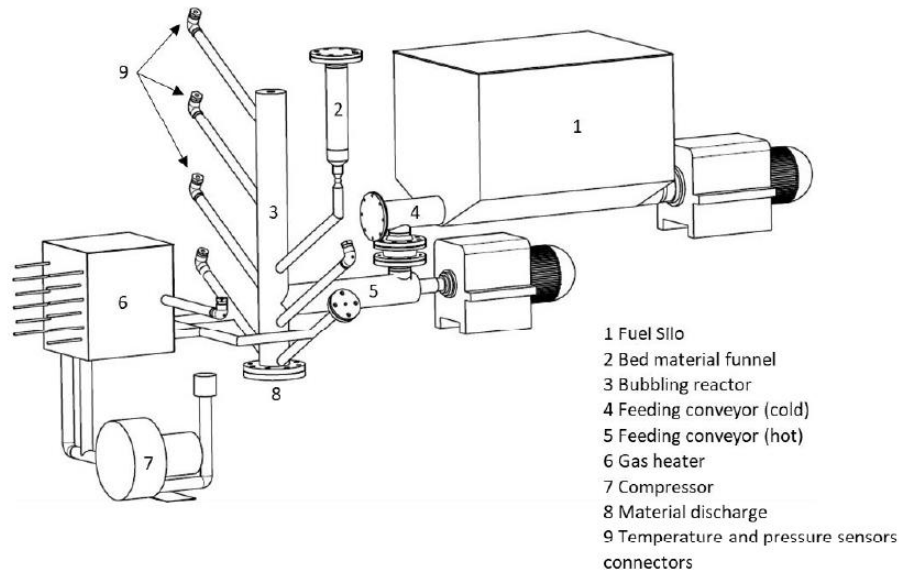


Figure 4-3. Pilot-scale BFB gasifier with auxiliary connections

The reactor operates at atmospheric pressure and in a bubbling fluidization regime. The diameter, height and wall thickness are 0.1 m, 1 m, and 0.004 m respectively. The inner surface of the reactor is insulated with thick fiberglass, while the exterior surface is coated with refractory material. The product gases from the experiments were combusted in the chimney. Three 3KW electrical heaters are used in this configuration, one to heat the gasifying agent in the gas heater (6) and the other two to heat the reactor. The reactor (3), biomass storage - silo (1), biomass feeding screws (4 and 5) and bed material funnel (2) are shown in Figure 4-3.



Figure 4-4. BFB gasification reactor at USN, Porsgrunn

A compressor provides the gasifying air, which is heated before entering the reactor. During the experiments, the airflow rate is measured using a BROOK air flowmeter and manually controlled. The air preheater raises the temperature of the gasifying air to roughly 450°C. The fuel is kept in a sealed silo and transported to the reactor via two screw conveyors. The cold screw conveyor is connected to the hot screw conveyor through a non-conductive flange to prevent heat transfer from the reactor to the silo. The flange functions as a biomass bridge, preventing a fire/heat from spreading backwards into the silo. The biomass feed rate is controlled by altering the cold screw motor's speed or operating time. During reactor operation, the hot screw motor runs continuously. Biomass is fed at a height of 0.25 m above the air distributor.

There are four pressure and temperature sensors installed along the reactor. The additional pressure and temperature sensors are installed at the air preheater, the air inlet, the gas

outlet, the silo, the screw conveyors, and the reactor heaters. The gauge pressure at the given point is measured by the pressure sensor. A programmable logic controller (PLC) is used to collect data and control parameters, and it is connected to a computer running the LabVIEW program. The reactor heater and air preheater have default cut-off temperatures of 1000°C and 600°C, respectively. During the experiment, a constant nitrogen flow of 0.5 L/min is maintained through the silo to prevent any gas movements from the reactor to the silo. In the event of an emergency shutdown, an additional nitrogen supply line is kept on standby condition to flush the reactor. Sensors for the detection of H₂, CO, and N₂ are also installed at the site to detect any gas leaks. The produced gas is mixed with propane (if required) and burned in a ventilated chimney.

4.4 Gas sampling

The temperature and pressure along the reactor were recorded constantly at one-second intervals. Three samples were taken at each air flow rate to reduce measurement uncertainty. The gas samples were taken at roughly 10-minute intervals. 25 ml syringes were used to collect the gas samples, which were then analyzed in an SRI 86110C gas chromatography (GC) with a thermal conductivity detector. The GC used for the gas analysis is shown in Figure 4-5.



Figure 4-5. SRI gas chromatography

The GC contains a packed molecular size 13x column for N₂, O₂, CO, and CH₄ detection, as well as a silica gel packed column for CO₂ detection. The GC uses helium as a carrier gas, and the concentration of H₂ was determined using the difference method. At lower concentrations,

helium does not reliably predict H₂ compositions. The accuracy of the estimated H₂ concentration was confirmed by using nitrogen as the carrier gas in the gas chromatograph.

4.5 CPFD Simulation Setup

Barracuda VR software was used to create a CPFD model to simulate the gasification process. The reactor was designed as an open cylinder with a 100 mm diameter and a 1000 mm height. The Wen-Yu drag model was chosen with 70% momentum loss after a normal to wall particle collision and 1% momentum loss after a tangent to wall particle collision. The normal and tangential coefficients represent the fraction of the particle momentum that is preserved after impact with the wall [43]. The developed geometry was divided into 8800 computational cells. Figure 4-6 shows the boundary conditions, computational grid, and the initial particle in the bed. Table 4-2 gives an overview of the initial and the boundary conditions for the CPFD model.

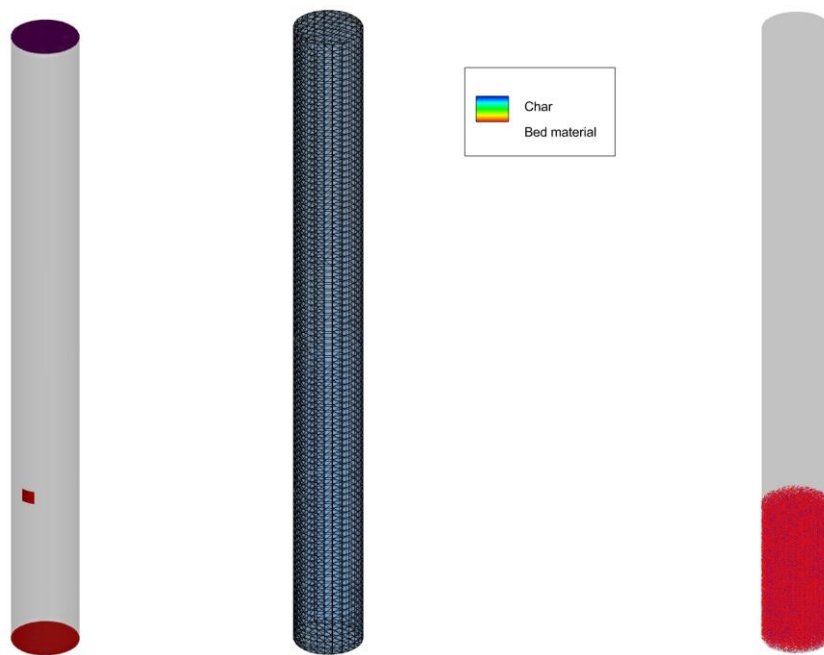


Figure 4-6. Schematic illustration of the barracuda model, (a) Boundary conditions, (b) Computational grid, (c) Initial particle in the bed.

Table 4-2. Initial and boundary conditions

Material	Initial conditions	Boundary conditions
Air	<ul style="list-style-type: none">• 101325 Pa	<ul style="list-style-type: none">• 101325 Pa• 500 K• 5 kg/hr
Sand (Silica)	<ul style="list-style-type: none">• 101325 Pa• Particle size: 850-1000 μm• Height: 200 mm• Density: 2650 kg/m^3• Volume fraction: 0.5	
Biomass (Lignin)		<ul style="list-style-type: none">• 101325 Pa• 500K• Particle feed ON• 3.75 kg/hr
Product gas		<ul style="list-style-type: none">• 101325 Pa• No particle exit

5 Results and discussion

5.1 Experimental results

A cold flow model experiment was done with sand as the bed material to study the flow behavior and particle segregation. The pressure drop profiles with respect to superficial gas velocity for the selected bed material is presented in Figure 5-1.

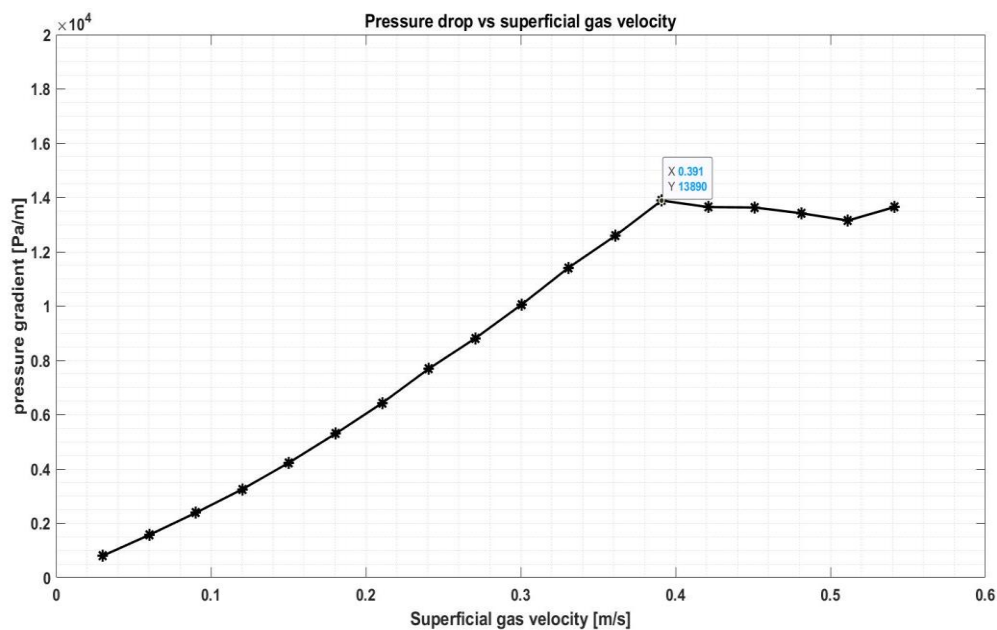


Figure 5-1. Pressure gradient profile for bed material.

The pressure drop increases initially with the increase of gas velocity. Then it reaches a peak, and then remains almost constant. The minimum fluidization velocity is 0.39 m/s for the selected bed material and the pressure drop at the minimum fluidization condition is 13890 Pa/m.

Sieve analysis was done to select the bed material of a particular size range. Sand particles in the size range of 850 μm – 1000 μm were chosen for the the BFB gasifier experiments. Figure 5-2 illustrates the process of sieve analysis and the particle range (shaded with light blue) used for the experiments.

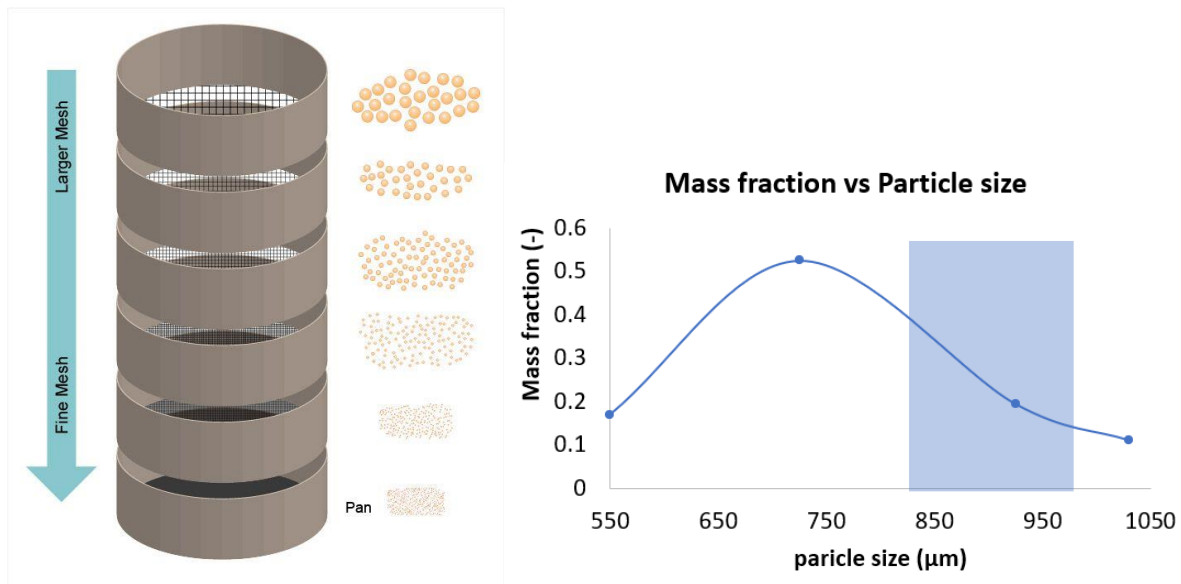


Figure 5-2. Sieve analysis process and the particle size profile for the bed material.

The minimum fluidization velocity obtained from the cold flow model experiments was used as a basis for BFB gasifier experiments. It is important to be within the bubbling fluidization regime at the reactor operating conditions. Therefore, the minimum fluidization velocity was recalculated for hot bed conditions using the minimum fluidization velocity obtained from the cold flow model experiment. An excess supply of air may add more oxygen which can shift the conversion process into combustion. Also, additional heat is needed to heat up the excess air which can cause the reduction of conversion efficiency. That is why it is important to obtain the minimum fluidization velocity from a cold flow model which ensures good mixing and heat transfer [44].

The temperature and pressure inside the gasification reactor fluctuate because of various physical and chemical transformations. The temperature inside the bed and the pressure at the reactor wall of the bubbling fluidized bed gasifier during the experiments are presented in Figure 5-3. In comparison to the pressure in the reactor, the temperature fluctuates more. This is primarily due to irregular biomass feeding through the screw conveyor. Irregular biomass feeding affects the ER which change the reaction mechanism. A high biomass content favors partial oxidation, while a low biomass content favors total oxidation causing the rise of the reactor temperature [43].

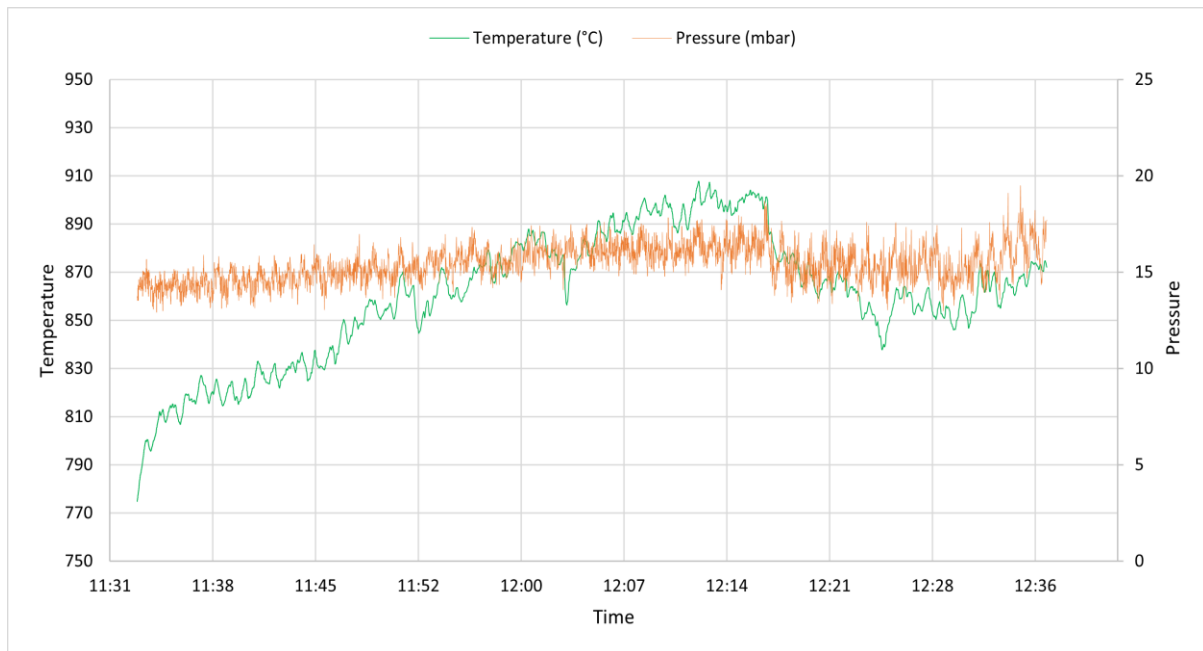


Figure 5-3. Temperature and pressure inside the reactor

Experiments were done with lignin pellets and air in the bubbling fluidized bed reactor. The average product gas composition from the experiment is presented in Figure 5-4. With an increase of ER, the production of N_2 , and CO_2 increase whereas, the amount of CH_4 , CO and H_2 decrease noticeably. The amount of O_2 remains almost the same during the process. The increase in CO_2 yield is noticed with the increase in ER. The decrease of CO and H_2 can be the result of a deficient amount of O_2 and lower reaction rate. This leads to an increase in N_2 in the product gas. However, the required final product gas composition can be obtained using various combinations of ER for lignin. The gasifier performance is presented in Table 5-1.

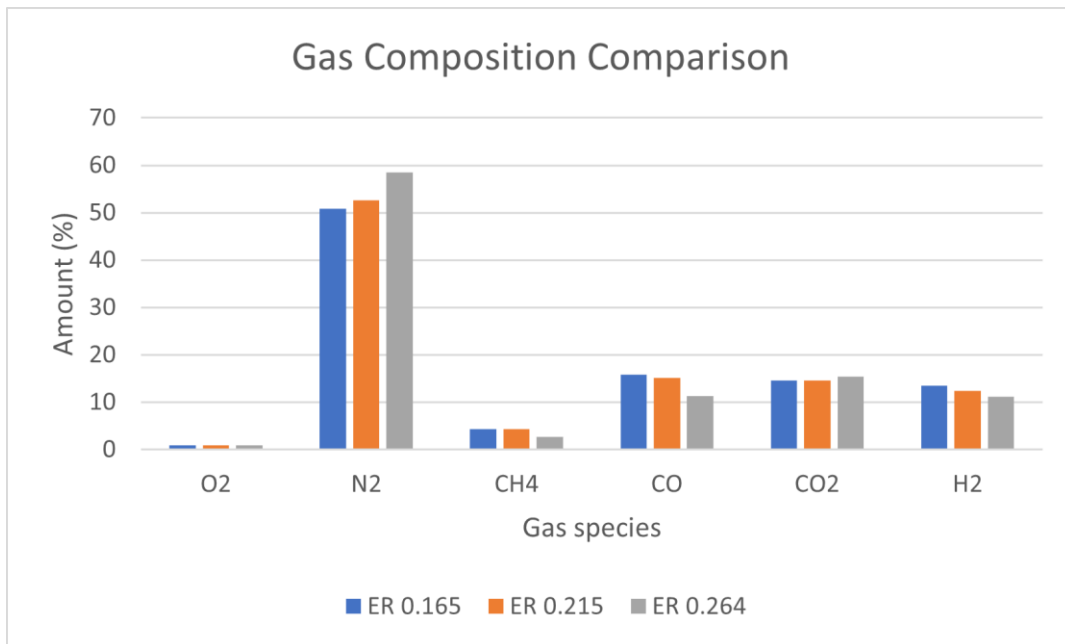


Figure 5-4. Product gas composition from experiment

Table 5-1. Gasification performance indicator for lignin pellets

ER	0.165	0.215	0.264
Product gas (Nm³/hr)	5.74	7.25	8.03
Gas yield (Nm³/kg biomass)	1.53	1.93	2.14
LHV (MJ/Nm³)	4.95	4.8	3.61
CCE (%)	40.3	39.8	34.4
CGE (%)	42.14	51.6	42.98
Energy rate (MJ/hr)	28.41	34.8	28.99

The product gas and the yield increased with the increase of the equivalence ratio. The LHV of product gas decreased with an increase in ER. CCE changes noticeably with the change of ER. It decreases with the increase of ER. This is probably because of the dilution of product gas with N_2 .

5.2 Simulation results

Simulations were performed with Barracuda VR 21.1.1 and the gas composition and flow rates were monitored. The air flow rate was taken as 5 kg/hr and the mass flow rate of lignin was taken as 3.75 kg/hr. Figure 5-5 shows the mole fractions of CH_4 , CO and H_2 along with the height of the reactor.

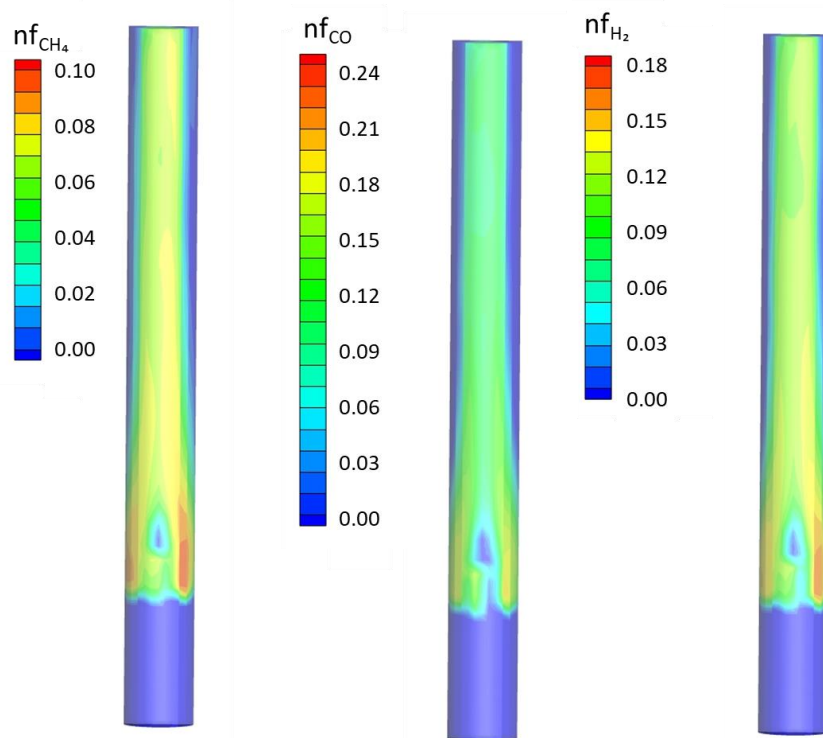


Figure 5-5. Gas composition along the reactor

There are no noticeable differences up to the biomass feeding position. This signifies that the char gasification/oxidation is less significant than the homogeneous reaction inside the bed. Different gas compositions result from devolatilization and chemical changes of biomass inside the bed. This demonstrates that the chemical reactions as well as the bed

hydrodynamics in a bubbling fluidized bed reactor, play an important role in the product gas quality and quantity. The optimized reactor's operation would result in uniform particle distribution and operates in the bubbling fluidization regime. Figure 5-6 and Figure 5-7 illustrate the particle volume fraction and the fluid temperature distribution along the reactor after 50 seconds of simulation.

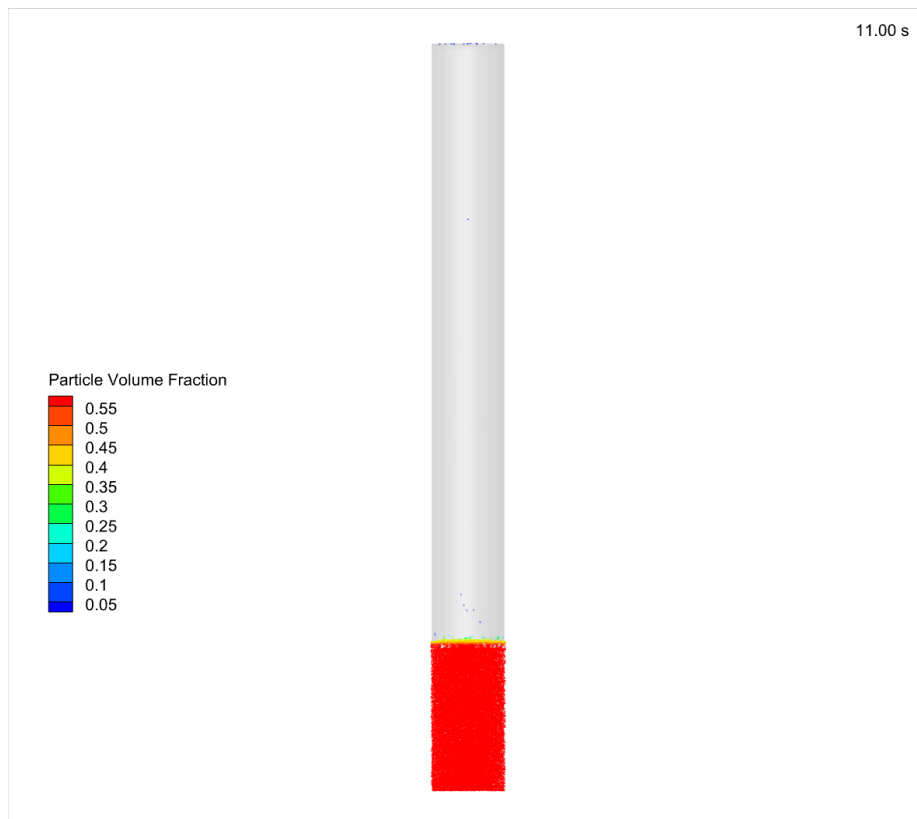


Figure 5-6. Particle volume fraction at simulation bed hydrodynamics at 50 s

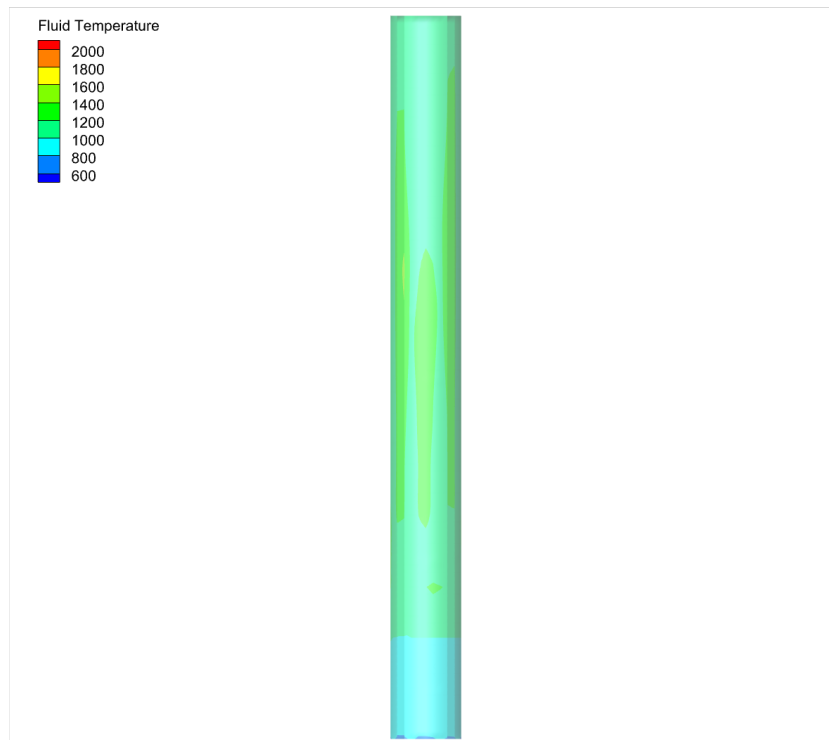


Figure 5-7. Fluid temperature at simulation bed hydrodynamics at 50 s

The system reaches a steady state after around 15 seconds of simulation time. Figure 5-8 depicts the gas composition as a function of simulation time. Production of CO₂ increases after 6 seconds of simulation time. The high fraction of CO₂ shortly after startup represents the combustion process as there is extra oxygen present inside the reactor. Between 5-10 seconds of simulation time, production of CH₄, CO and H₂ started progressively which clearly indicates that the combustion process is gradually shifting towards gasification. The gas generation rate at steady state varies around its mean value due to the various physical and chemical transformations that take place within the reactor.

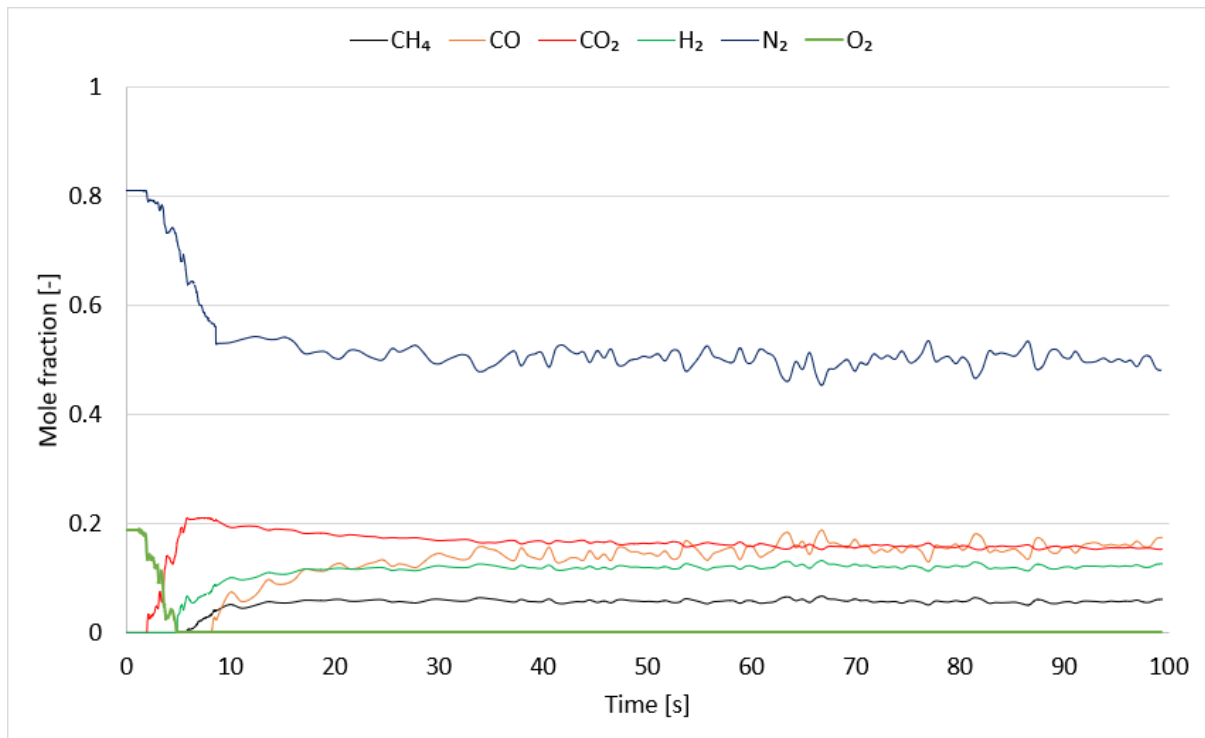


Figure 5-8. Product gas properties with respect to time

5.3 Comparative analysis

The average gas composition from experimental results can be compared with the simulation results as shown in Figure 5-9. Though various reactions take place during the gasification process, minor reactions are not included in the barracuda simulations. They usually take up a lot of computer resources and time. That can be a reason for noticing some dissimilarities between the results. During the simulation, the average oxygen concentration was zero, whereas during the experiment, oxygen concentration was roughly 1% of the overall volume composition. The samples were obtained in a syringe for the gas analysis and this can be the cause of such variation.

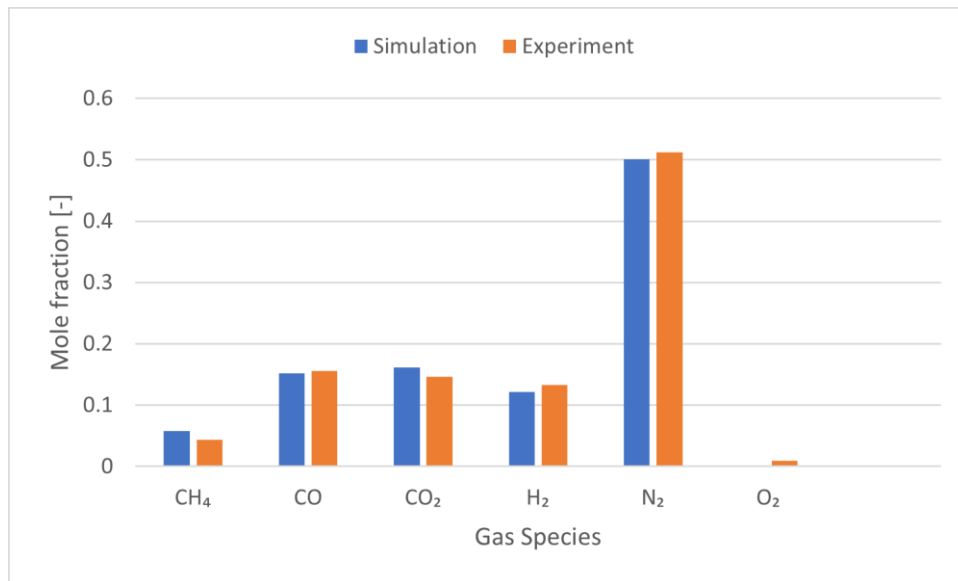


Figure 5-9. Comparison of average gas species at ER = 0.165

The results obtained from the gasification of lignin pellets can also be compared with the results obtained from the gasification of wood pellets performed by Ramesh et al. [24]. Both sets of experiments were performed at the pilot scale gasifier located at USN. Though they are not directly comparable because of different operating conditions, the study can give a clear overview of the gasification for the considered pellets in a BFB gasifier. Table 5-2 illustrates the comparative analysis between the product gases of the two experiments at ER of 0.26. The wood pellets gasification gave comparatively good product gas composition compared to lignin pellets. The CCE is 55.1% for wood pellets whereas it is 34.4% for lignin for the same equivalence ratio of 0.26.

Table 5-2. Product gas composition for wood pellets and lignin gasification

Gas component	Wood pellets (%)	Lignin (%)
CO	14.24	11.33
H ₂	17.66	11.18
CO ₂	15.17	15.43
O ₂	0.93	0.91
N ₂	52.00	58.44

6 Conclusion

With the growing importance of climate change, the industry has been committed to sustainable development. Gasification of biomass is an approach that drives the global market with its versatility. This thesis is focused on the gasification of lignin pellets, an underutilized byproduct from different industrial processes. The main objective of the project was achieved in this study.

Primarily, lignin gasification was the major focus of this study. Several literature studies were accomplished in this work to get an overview of lignin production, applications and conversion. Experimental studies were performed in a cold flow model of a BFB reactor and a pilot-scale BFB gasifier. The minimum fluidization velocity was investigated using the cold flow model. The selected bed material had a minimum fluidization velocity of 0.39 m/s. The selected bed material was in the range of 850 μm to 1000 μm . Gasification experiments were performed for lignin pellets at different air flow rates of 5 kg/hr (ER = 0.165), 6.5 kg/hr (ER = 0.215) and 8 kg/hr (ER = 0.264) with the biomass flow rate of 3.75 kg/hr in the BFB gasifier. Based on the mass balance of N_2 in the inlet and outlet gas, the product gas flow rate and the gasifier performance were analyzed. The results gave a complete overview of the gasifier performance for the lignin pellets. The gasifier performance was analyzed in terms of product gas yield (GY), LHV, CCE, CGE and energy rate. Gasification of lignin pellets gave a carbon conversion in the average range of 38%.

For the gasification of lignin in the pilot-scale BFB gasifier, CPFD models were developed. The model is based on the conservation of mass, momentum, and energy. Experimental data was used to validate the models.

The overall result shows that the product gas has the potential to be used directly in heat and power generation. To obtain high quality product gas, appropriate for biofuels and chemicals synthesis, biomass gasification with steam/oxygen or utilizing a DFB gasifier is recommended. For lignin pellet gasification, catalytic bed material is suggested to have a higher carbon conversion for lignin pellets gasification.

References

1. Guo, N., *Modelling of reacting multi-phase flow for biomass gasification*. 2020.
2. Matas Güell, B., J. Sandquist, and L. Sørum, *Gasification of biomass to second generation biofuels: a review*. Journal of Energy Resources Technology, 2013. **135**(1).
3. Haryanto, A., et al., *Upgrading of syngas derived from biomass gasification: A thermodynamic analysis*. Biomass and bioenergy, 2009. **33**(5): p. 882-889.
4. International, B. *Lignin pellets – from residual product to valuable biofuel*. 2020, May 25; Available from: <https://bioenergyinternational.com/lignin-pellets-from-residual-product-to-valuable-biofuel/>.
5. Bandara, J., B.M.E. Moldestad, and M.S. Eikeland, *Analysing the effect of temperature for steam fluidized-bed gasification of biomass with MP-PIC simulation*. 2018.
6. Bridgwater, A., *The technical and economic feasibility of biomass gasification for power generation*. Fuel, 1995. **74**(5): p. 631-653.
7. Basu, P., *Biomass gasification, pyrolysis and torrefaction: practical design and theory*. 2018: Academic press.
8. Timsina, R., et al., *Simulation of air-biomass gasification in a bubbling fluidized bed using CPFD model*. 2019.
9. Parmar, K., *Biomass-An overview on composition characteristics and properties*. IRA-International journal of applied sciences, 2017. **7**(1): p. 42-51.
10. Ragauskas, A.J., et al., *Lignin valorization: improving lignin processing in the biorefinery*. science, 2014. **344**(6185): p. 1246843.
11. Hatakeyama, H. and T. Hatakeyama, *Lignin structure, properties, and applications*, in *Biopolymers*. 2009, Springer. p. 1-63.
12. Gellerstedt, G. and G. Henriksson, *Lignins: major sources, structure and properties*. Monomers, polymers and composites from renewable resources, 2008: p. 201-224.
13. Gosselink, R., et al., *Co-ordination network for lignin—standardisation, production and applications adapted to market requirements (EUROLIGNIN)*. Industrial Crops and Products, 2004. **20**(2): p. 121-129.
14. Holladay, J.E., et al., *Top value-added chemicals from biomass-Volume II—Results of screening for potential candidates from biorefinery lignin*. 2007, Pacific Northwest National Lab.(PNNL), Richland, WA (United States).
15. Saito, T., et al., *Methanol fractionation of softwood kraft lignin: Impact on the lignin properties*. ChemSusChem, 2014. **7**(1): p. 221-228.
16. Sannigrahi, P., Y. Pu, and A. Ragauskas, *Cellulosic biorefineries—unleashing lignin opportunities*. Current Opinion in Environmental Sustainability, 2010. **2**(5-6): p. 383-393.

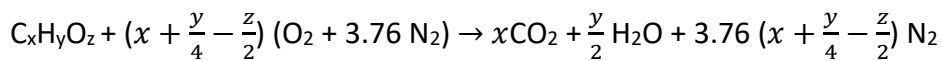
17. Poveda-Giraldo, J.A., J.C. Solarte-Toro, and C.A.C. Alzate, *The potential use of lignin as a platform product in biorefineries: A review*. Renewable and Sustainable Energy Reviews, 2021. **138**: p. 110688.
18. Timsina, R., *Modelling and simulations of bubbling fluidized bed and entrained flow biomass gasification reactors*. 2022.
19. Campoy, M., et al., *Air– steam gasification of biomass in a fluidized bed under simulated autothermal and adiabatic conditions*. Industrial & engineering chemistry research, 2008. **47**(16): p. 5957-5965.
20. Campoy, M., et al., *Air–steam gasification of biomass in a fluidised bed: Process optimisation by enriched air*. Fuel Processing Technology, 2009. **90**(5): p. 677-685.
21. Liakakou, E., et al., *Gasification of lignin-rich residues for the production of biofuels via syngas fermentation: Comparison of gasification technologies*. Fuel, 2019. **251**: p. 580-592.
22. Liakakou, E., et al., *Connecting gasification with syngas fermentation: Comparison of the performance of lignin and beech wood*. Fuel, 2021. **290**: p. 120054.
23. Furuvik, N.C.I., R. Jaiswal, and B.M.E. Moldestad, *Comparison of experimental and computational study of the fluid dynamics in fluidized beds with agglomerates*. 2020.
24. Timsina, R., et al., *Experimental Evaluation of Wood and Grass Pellets in a Bubbling Fluidized Bed Gasifier*. Available at SSRN 4034170.
25. Qin, K., et al., *High-temperature entrained flow gasification of biomass*. Fuel, 2012. **93**: p. 589-600.
26. Gómez-Barea, A. and B. Leckner, *Modeling of biomass gasification in fluidized bed*. Progress in Energy and Combustion Science, 2010. **36**(4): p. 444-509.
27. Franco, C., et al., *The study of reactions influencing the biomass steam gasification process* ☆. Fuel, 2003. **82**(7): p. 835-842.
28. Gungor, A. and U. Yildirim, *Two dimensional numerical computation of a circulating fluidized bed biomass gasifier*. Computers & Chemical Engineering, 2013. **48**: p. 234-250.
29. Bin, C., et al., *Investigation of gas-solid two-phase flow across circular cylinders with discrete vortex method*. Applied Thermal Engineering, 2009. **29**(8-9): p. 1457-1466.
30. Ku, X., T. Li, and T. Løvås, *CFD–DEM simulation of biomass gasification with steam in a fluidized bed reactor*. Chemical Engineering Science, 2015. **122**: p. 270-283.
31. Chen, C., et al., *CPFD simulation of circulating fluidized bed risers*. Powder technology, 2013. **235**: p. 238-247.
32. Snider, D.M., S.M. Clark, and P.J. O'Rourke, *Eulerian–Lagrangian method for three-dimensional thermal reacting flow with application to coal gasifiers*. Chemical engineering science, 2011. **66**(6): p. 1285-1295.
33. Patel, M., K. Pericleous, and M. Cross, *Numerical modelling of circulating fluidized beds*. International Journal of Computational Fluid Dynamics, 1993. **1**(2): p. 161-176.
34. Zanzi, R., K. Sjöström, and E. Björnbom, *Rapid pyrolysis of agricultural residues at high temperature*. Biomass and Bioenergy, 2002. **23**(5): p. 357-366.

35. Ku, X., T. Li, and T. Løvås, *Eulerian–Lagrangian simulation of biomass gasification behavior in a high-temperature entrained-flow reactor*. *Energy & fuels*, 2014. **28**(8): p. 5184-5196.
36. Bates, R.B., et al., *Steam-air blown bubbling fluidized bed biomass gasification (BFBBG): Multi-scale models and experimental validation*. *AIChE Journal*, 2017. **63**(5): p. 1543-1565.
37. Xie, J., et al., *Eulerian–Lagrangian method for three-dimensional simulation of fluidized bed coal gasification*. *Advanced Powder Technology*, 2013. **24**(1): p. 382-392.
38. Thapa, R., B. Halvorsen, and C. Pfeifer, *Modeling of reaction kinetics in bubbling fluidized bed biomass gasification reactor*. *International Journal of Energy and Environment (Print)*, 2013. **5**.
39. Rauch, R., J. Hrbek, and H. Hofbauer, *Biomass gasification for synthesis gas production and applications of the syngas*. *Wiley Interdisciplinary Reviews: Energy and Environment*, 2014. **3**(4): p. 343-362.
40. Lau, F., *Techno economic analysis of hydrogen production by gasification of biomass*. 2002, Golden Field Office, Golden, CO (US).
41. Soukup, G., et al., *In situ CO₂ capture in a dual fluidized bed biomass steam gasifier–bed material and fuel variation*. *Chemical Engineering & Technology: Industrial Chemistry-Plant Equipment-Process Engineering-Biotechnology*, 2009. **32**(3): p. 348-354.
42. Van Der Laan, G.P. and A. Beenackers, *Kinetics and selectivity of the Fischer–Tropsch synthesis: a literature review*. *Catalysis Reviews*, 1999. **41**(3-4): p. 255-318.
43. Timsina, R., et al., *Experiments and computational particle fluid dynamics simulations of biomass gasification in an air-blown fluidized bed gasifier*. *International Journal of Energy Production and Management*. 2020. Vol. 5. Iss. 2, 2020. **5**(2): p. 102-114.
44. Jaiswal, R., et al., *Method of identifying an operating regime in a bubbling fluidized bed gasification reactor*. 2020.

Appendices

Appendix A: Calculation of ER for lignin pellets based on air flow rates

Stoichiometric combustion:



Molecular formula of lignin: **CH_{1.14}O_{0.35}** (C₈₁H₉₂O₂₈)

Fuel air ratio (FAR) at stoichiometric condition,

$$\begin{aligned} f_s &= \frac{m_f}{m_a} \Big|_{stoichiometric} \\ &= \frac{nM_f}{nM_a} \\ &= \frac{12 + 1 \times 1.14 + 16 \times 0.35}{1.11 \times 32 + 3.76 \times 1.11 \times 28} \\ &= 0.124 \end{aligned}$$

Therefore, air fuel ratio (AFR) will be $\frac{1}{f_s} = 8.075$. This implies that around 8.075 kg of air is needed for the complete combustion of 1 kg of lignin pellets.

For 5 kg/hr air flow rate, the ER = $\frac{5}{8.075 \times 3.75} = 0.165$.

Similarly, for 6.5 kg/hr and 8 kg/hr air flow rate, the ER is 0.214 and 0.264 respectively.

Appendix B: Formulation of Lower heating value (LHV), Gas yield (GY), Carbon conversion efficiency (CCE), and Cold gas efficiency (CGE)

$$\text{LHV (MJ/m}^3\text{)} = \{[\text{H}_2] * 107.98 + [\text{CO}] * 126.36 + [\text{CH}_4] * 358.18\} / 1000$$

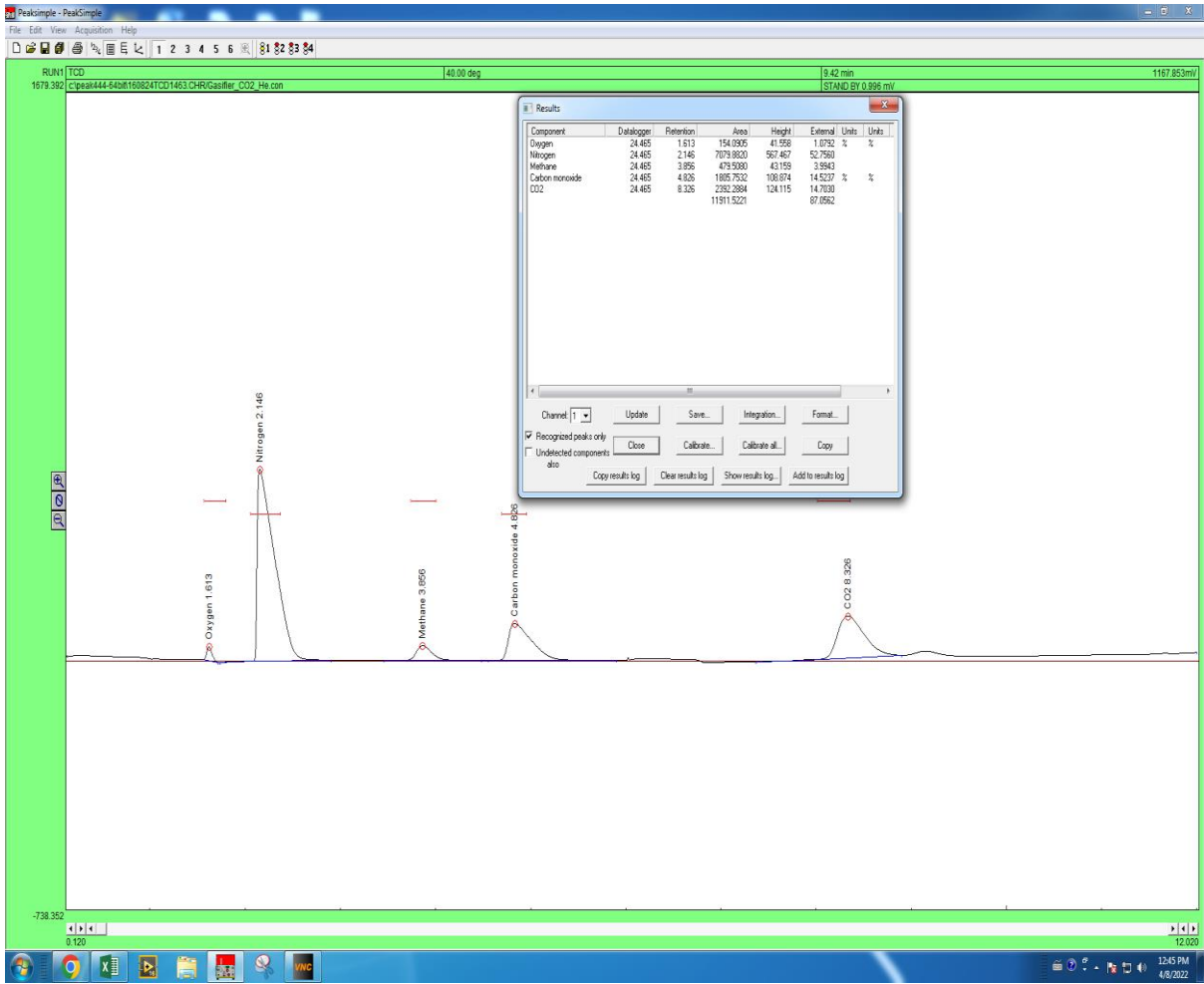
$$\text{GY} = \frac{\text{Volume flow of product gas } (\frac{\text{Nm}^3}{\text{h}})}{\text{Biomass feed rate } (\frac{\text{kg}}{\text{h}})}$$

$$\text{CCE}(\%) = \frac{12(\text{CO}\% + \text{CO}_2\% + \text{CH}_4\% + 2 * \text{C}_2\text{H}_4\%) * \text{GY}}{22.4 * \text{fuel C}\% * 100} 100\%$$

$$\text{CGE}(\%) = \frac{\text{LHV}_{\text{syngas}} * \text{GY}}{\text{LHV}_{\text{biomass}}} 100\%$$

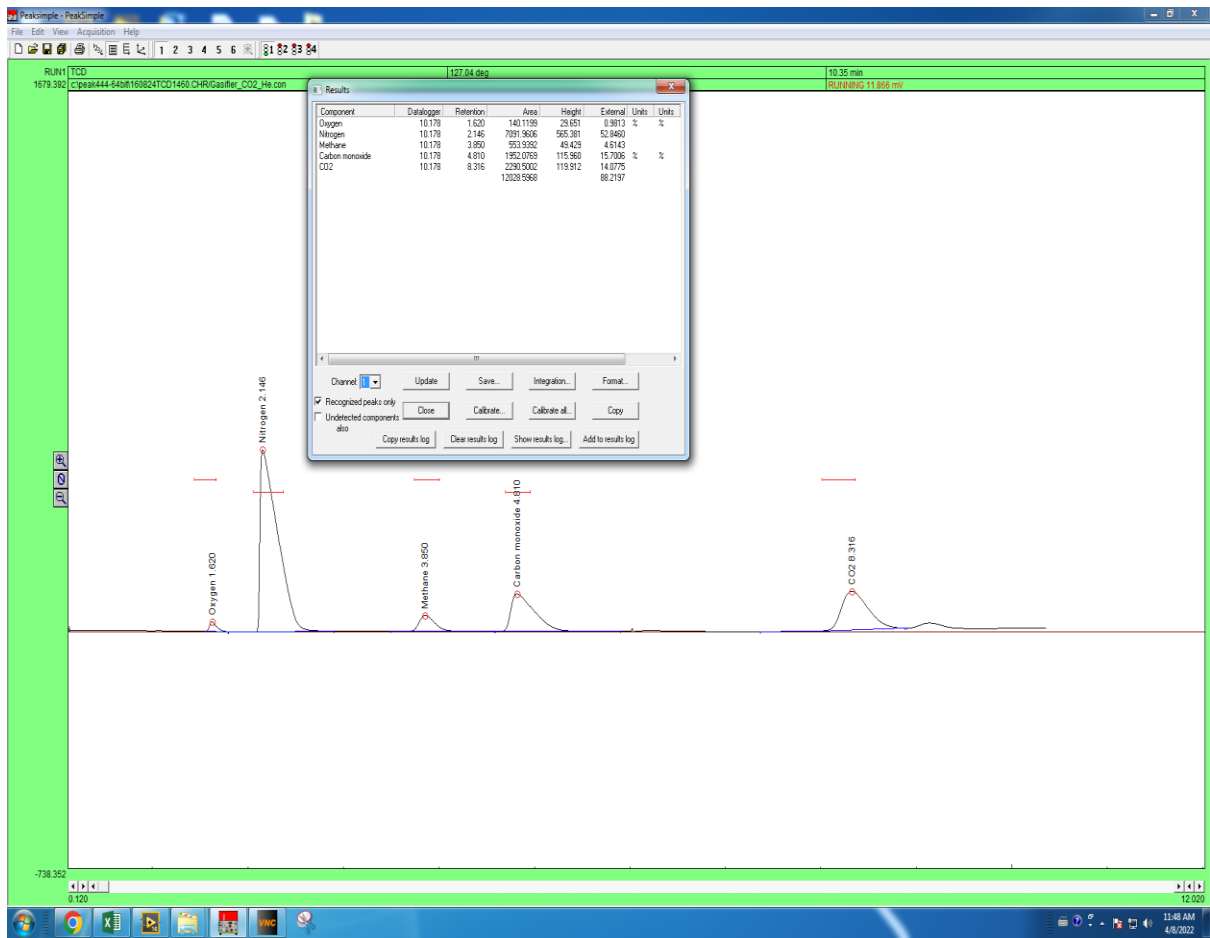
Appendix C: Gas chromatograph analysis

For 5 kg/hr at 12:09 PM



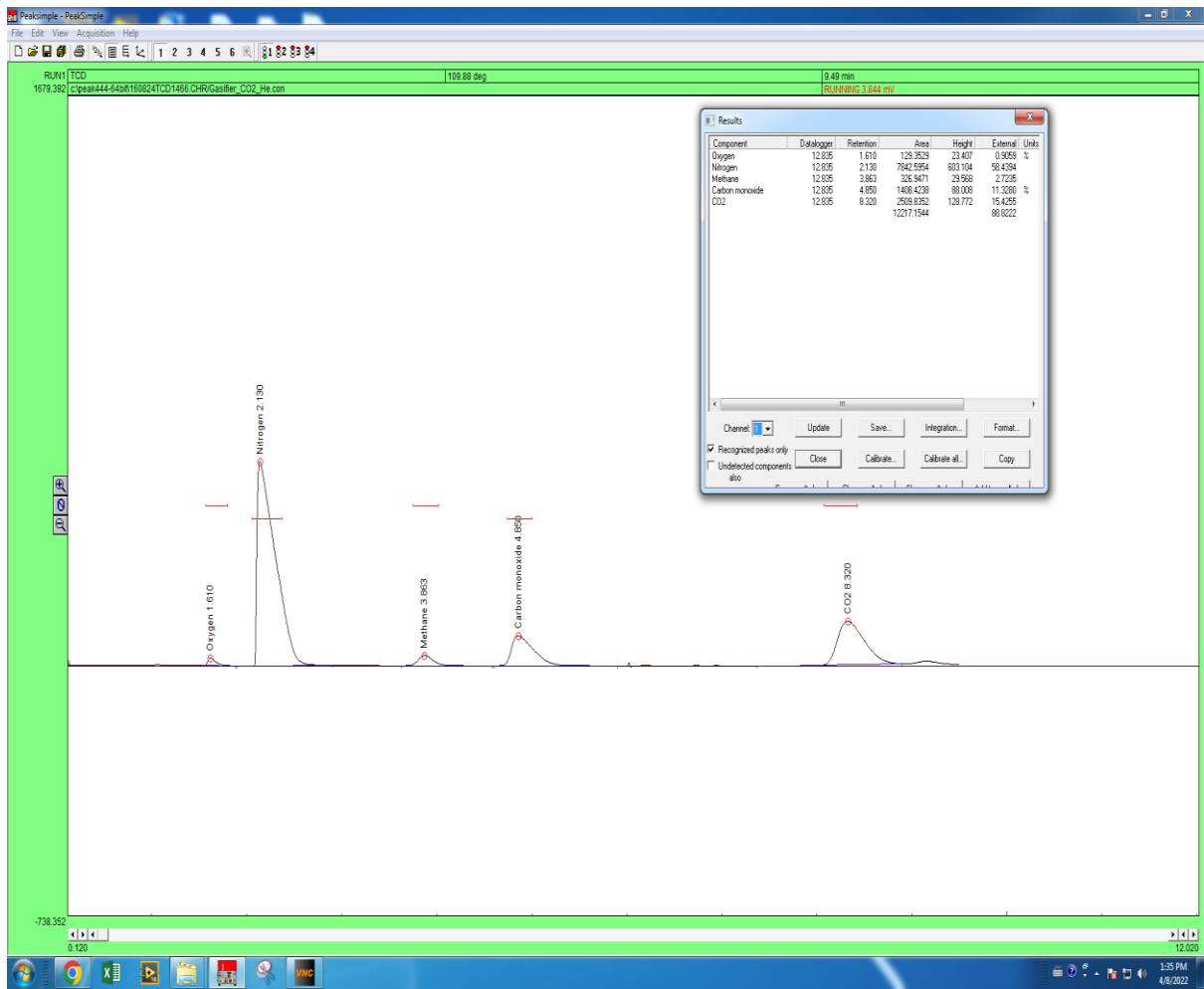
Component	Datalogger	Retention	Area	Height	External	Units	Units
Oxygen	24.465	1.613	154.0905	41.558	1.0792	%	%
Nitrogen	24.465	2.146	7079.8820	567.467	52.7560		
Methane	24.465	3.856	479.5080	43.159	3.9943		
Carbon monoxide	24.465	4.826	1805.7532	108.874	14.5237	%	%
CO2	24.465	8.326	2392.2884	124.115	14.7030		
			11911.5221		87.0562		

For 6.5 kg/hr at 11:36 AM



Component	Datalogger	Retention	Area	Height	External	Units	Units
Oxygen	10.178	1.620	140.1199	29.651	0.9813	%	%
Nitrogen	10.178	2.146	7091.9606	565.381	52.8460		
Methane	10.178	3.850	553.9392	49.429	4.6143		
Carbon monoxide	10.178	4.810	1952.0769	115.960	15.7006	%	%
CO2	10.178	8.316	2290.5002	119.912	14.0775		
			12028.5968		88.2197		

For 8 kg/hr at 12:36 PM



Component	Datalogger	Retention	Area	Height	External	Units
Oxygen	12.835	1.610	129.3529	23.407	0.9059	%
Nitrogen	12.835	2.130	7842.5954	603.104	58.4394	
Methane	12.835	3.863	326.9471	29.568	2.7235	
Carbon monoxide	12.835	4.850	1408.4238	88.008	11.3280	%
CO2	12.835	8.320	2509.8352	128.772	15.4255	
			12217.1544		88.8222	

Appendix D: Task description



Faculty of Technology, Natural Sciences and Maritime Sciences, Campus Porsgrunn

FMH606 Master's Thesis

Title: Experimental and computational study gasification of lignin pellets in a bubbling fluidized bed reactor.

USN supervisor: Ramesh Timsina, Britt M. E. Moldestad

External partner: SINTEF Energy

Task background:

The energy produced from sustainable sources plays an important role in achieving net-zero emissions, as promised by several countries across the globe by 2050. Gasification of biomass is a promising energy conversion technology of lignocellulosic biomass and other sustainable biomass substances. Fluidized beds are used to convert the biomass into a syngas. The syngas consists mainly of hydrogen (H_2), Carbon monoxide (CO) and Carbon dioxide (CO_2) and can further be converted into biofuels. Fluidized bed gasifiers are noted for their uniform heating, easy thermal control and high productivity. Owing to the uniformly and relatively low temperature in the fluidized bed gasifiers, a wide range of fuels can be used in the gasification reactor. Lignocellulosic biorefineries across the globe are able to convert cellulose and hemicellulose into higher valued chemicals and biofuels. However, lignin from the lignocellulosic biomass is an underutilized biorefinery waste. The lignin waste from the biorefinery will be used in the gasification experiments. To improve the efficiency of these gasifiers, it is necessary to get a better understanding of the operating parameters. Experimental and computational studies of the gasification process provide the optimal parameters for efficiency improvements.

Task description:

- Literature survey on:
 - Bubbling fluidized bed biomass gasification process.
 - Lignin produced from biorefineries – properties, global production amounts and other possible applications.
- Experimental studies of the lignin pellets using the gasification reactor located at USN.
- Analysis of the produced syngas (heating value and carbon conversion) obtained from the experiment in task 2.
- Analysis of gas composition, heating value and carbon conversion and compared with other biomasses.
- Develop a Computational Particle Fluid Dynamic (CPFD) model to simulate the same process in Barracuda VR.


Student category: PT or EET students

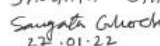
The task is suitable for students not present at the campus (e.g. online students): No

Practical arrangements:

A 20 kW biomass gasifier is installed at USN, Porsgrunn. The gasifier is designed to handle either air or steam as the gasifying agent and to operate under a bubbling fluidized bed regime. The rig is equipped with a gas chromatograph (GC) to analyse the composition of the product gas. The experiments planned in this study will be performed in this rig. The CPFD software Barracuda VR will be provided to use in the computer lab located at USN, Porsgrunn.

Signatures:

Supervisor (date and signature):  27.01.22

Student (write clearly in all capitalized letters + date and signature): SAUGATA GHOSH

27.01.22

Address: Kjalnes ring 56, NO-3918 Porsgrunn, Norway. Phone: 35 57 50 00 Fax: 35 55 75 47